SUPPLEMENTARY INFORMATION

The inoculum effect and band-pass bacterial response to periodic antibiotic treatment

Cheemeng Tan[1+,$], Robert Phillip Smith[1+], Jaydeep K. Srimani[1], Katherine A. Riccione[1], Sameer Prasada[1], Meta Kuehn[2], and Lingchong You[1,3,4*]

[1]Department of Biomedical Engineering, Duke University, Durham, NC 27708, USA

[2]Department of Biochemistry, Duke University Medical Center, Durham, NC 27710, USA

[3]Institute for Genome Sciences and Policy, Duke University, Durham, NC 27708, USA

[4]Center for Systems Biology, Duke University, Durham, NC 27708, USA

[*]Correspondence and requests for materials should be addressed to Lingchong You. E-mail: you@duke.edu; Tel: 919-660-8408; Fax: 919-668-0795.

ADDITIONAL FOOTNOTES

[+]These authors contributed equally to this work.

[$]Current address: Ray and Stephanie Lane Center for Computational Biology, Carnegie Mellon University, Pittsburgh, PA 15213

CONTENTS

SUPPLEMENTARY METHODS

Supplementary Table S1: Characteristics of the antibiotics used in this study

Antibiotic	Class	Mode of action	Stimulates the heat shock response in *E. coli*?
Kanamycin*	Aminoglycosides	Binds to 30S subunit of the ribosome and causes mistranslation of mRNA.	Yes(Kohanski et al., 2008; Vanbogelen and Neidhardt, 1990)
Streptomycin*	Aminoglycosides	Similar to other aminoglycosides	Yes(Vanbogelen and Neidhardt, 1990)
Puromycin*	Aminonucleoside	Binds to 50S subunit of the ribosome and causes mistranslation of mRNA.	Yes(Vanbogelen and Neidhardt, 1990)
Gentamicin*	Aminoglycosides	Similar to other aminoglycosides	Shown in this study
Neomycin*	Aminoglycosides	Similar to other aminoglycosides	Shown in this study
Tobramycin*	Aminoglycosides	Similar to other aminoglycosides	Shown in this study
Nourseothricin*	Aminoglycosides	Similar to other aminoglycosides	Shown in this study
Chloramphenicol^	Chloramphenicol	Binds to 50S subunit of the ribosome, thereby inhibiting peptidyl transferase activity.	No(Vanbogelen and Neidhardt, 1990)
Tetracycline^	Tetracycline	Binds to 30S subunit of ribosome and inhibits translation by inhibiting aminoacyl tRNA binding to ribosome.	No(Vanbogelen and Neidhardt, 1990)

*** indicates bactericidal, ^ indicates bacteriostatic**

Strains, growth conditions, and medium

Unless otherwise noted, *Escherichia coli* strain BL21 (B F- *dcm ompT hsdS*(r_B- m_B-) *gal*) was used throughout this study. To prepare overnight cultures, we inoculated Luria-Bertani (LB) medium from a frozen BL21 glycerol stock. The overnight cultures were then diluted again at 100-fold into 3ml fresh LB medium and incubated overnight at 37^{o}C. M9 medium, supplemented with 0.4% (w/v) glucose and 0.1% (w/v) casamino acids, was used for growth assays. 200μl cultures overlayed with 50μl mineral oil (to prevent evaporation) were grown in a 96 well microplate (Victor 3 plate reader, Perkin Elmer, Massachusetts, USA) at 37^{o}C and shaken automatically at every 10 minutes. Optical density at 600nm was recorded at 10 minute intervals. Sulforhodamine, serine protease inhibitor 4-(2-aminoethyl) benzenesulfonyl fluoride hydrochloride, cysteine protease inhibitor E64, and aspartyl protease inhibitor Pepstatin were purchased from Sigma (Missouri, USA).

Unless otherwise noted, IE experiments were initiated by diluting an overnight culture 500-fold (low initial density, 2.6 x10^6 ± 5.7x10^5 CFU/mL) or 50-fold (high initial density, 4.1x10^7 ± 7.3x10^6 CFU/mL) into fresh M9 medium. For BW25113 *E. coli* strain (Fig. S4H-J), IE experiments were initiated by diluting an overnight culture 500-fold (low initial density) or 50000-fold (high initial density) into fresh M9 medium. Initial bacterial densities were controlled tightly by using the same preparation steps for all overnight cultures. The resulting cultures were then supplemented with varying concentrations of antibiotics and incubated in a plate reader at 37^{o}C for 24 hours. We note that extending our analysis to 28 hours did not affect our conclusion with chloramphenicol. Bacterial density was measured at 10 minute intervals.

Knockout strains of BW25113 (JW0428: *D(araD-araB)567,* Δ*lacZ4787(::rrnB-3), LAM-, rph-1,* Δ*(rhaD-rhaB)568, hsdR514, DclpX724::kan*; JW0429: *D(araD-araB)567,* Δ*lacZ4787(::rrnB-3), LAM-, rph-1,* Δ*(rhaD-rhaB)568, hsdR514, Dlon-725::kan,* JW3686-7: F-, *Δ(araD-araB)567*, *ΔlacZ4787*(::rrnB-3), *&lambda*$^-$, *rph-1,ΔtnaA739::kan*, *Δ(rhaD-rhaB)568, hsdR514,* JW2505-1: F-, *Δ(araD-araB)567*, *ΔlacZ4787*(::rrnB-3), *&lambda*$^-$, *rph 1,ΔsseA767::kan, Δ(rhaD-rhaB)568, hsdR514*) were obtained from the E. Coli Genetic Stock Center (CGSC).

Western blot (Supplementary Figure S1A and S3E)

An overnight culture was diluted 50-fold in 5mL of M9 medium and overlayed with 500µL of mineral oil. Cultures were incubated at 37^{o}C for 2 hours with either antibiotics at 10% MIC of the 50-fold dilution or without drugs. In addition, cultures were incubated at 42^{o}C without antibiotics. Cells were collected at 16,000 x g, resuspended in 100µl of lysis buffer (0.01M Tris & 4% (w/v) SDS, protease inhibitor) and lysed by vortexing for 30 seconds at full speed followed by 2 minutes on ice. This was repeated four times. Cell debris was removed by centrifugation at 16,000 x g at 4^{o}C for 20 minutes and total protein was determined using a Microplate BCA Protein Assay Kit (ThermoScientific, IL, USA). 10µg of total protein was subjected to SDS-PAGE and was transferred to nitrocellulose (Biorad, CA, USA) overnight at 4^{o}C. Immunoblots were blocked with 5% skim milk in 1% TBST for 2 hours. Blots were incubated with DnaK (1:10,000) antibody in 5% skim milk (TBST) for 1 hour, washed twice for 30 minutes in TBST and incubated with 1:2000 anti-mouse antibody (GE Healthcare, Buckinghamshire, UK) for 1 hour. Blots were washed twice for 30 minutes in TBST. For detection of MalE, blots were stripped with Restore PLUS Western Blot Stripping Buffer as recommended by the manufacturer (ThermoScientific). Detection of MalE was performed as

recommended by the manufacturer (New England Biolabs, MA, USA). Proteins were visualized using Amersham ECL Western Blotting Detection Reagents (GE Healthcare). Coomassie staining of duplicate gels was also performed concurrent to immunoblotting. DnaK density values were normalized by MalE density value. All densities were calculated using a box of fixed size using Adobe Photoshop (San Jose, CA). We note that while the DnaK antibody used in these experiments was raised specifically for *E. coli*, we infer that this antibody reacts to DnaK in *S. typhimurium.* The signal observed in proteins extracted from *S. typhimurium* was at the expected molecular weight of *S. typhimurium* DnaK (~69kDa) and DnaK proteins of both *E. coli* and *S. typhimurium* are 96.9% identical and 99.6% similar. We also found that the *E. coli* specific MalE antibody was not cross-reactive to *S. typhimurium* MalE. As such, duplicate Coomassie gels are presented as a loading control for these samples (Supplementary Figure S3E).

Pulse-chase type assays (Supplementary Figure S1B and S1C)

pTetCFPlaa plasmids (p15a, Amp) contain a P_{tet} promoter (Lutz and Bujard, 1997) that regulates the expression of a cyan fluorescent protein (CFP) fused to the SsrA-tag (*cfp-laa*). As a control, we also designed the same plasmid to express CFP without an SsrA-tag. An overnight culture of BL21Pro cells (*ompT, hsdS*$_B$*(*$r_B^- m_B^-$*), gal, dcm, F–*; containing *tetR,* P_{laci}^q*/laci*, and Sp^r on an autonomously replicating plasmid) carrying the pTetCFPlaa plasmids was diluted 100-fold into fresh M9 medium supplemented with ampicillin (100μg/ml) and 100ng/ml anhydrous tetracycline that induces the P_{tet} promoter. The culture was incubated for 8 hours at 37^{o}C and 250 rotations per minute. Next, the culture was spun down, washed with fresh M9 medium, and diluted 500-fold into 200μl fresh M9 medium, supplemented with the specified antibiotics and overlayed with 50μl mineral oil. The cultures were incubated in a plate reader at 37^{o}C. OD_{600}

and CFP intensity were recorded at 10 minute intervals. We note that synthesis rates were unlikely to impact the overall trend due to inhibition of mRNA translation by the antibiotics. To assess statistical significance, we calculated exponents of the fitted function exp^{kt}, which were used for paired t-tests. Indeed, based on such analysis, the exponents of the fitted curves (k) are significantly different between kanamycin and chloramphenicol (p-value=0.01). In contrast, chloramphenicol and 'Kan -ssrA' are not significantly different (p-value=0.7).

plac/araL13YFP plasmids (p15a, Amp) were constructed by substituting the T7 gene in the pTetT7EYFP plasmids (Tan et al., 2009) with the *rplM* gene (encoding ribosomal protein L13) amplified from the genome of wild type *E. coli* strain MG1655. Next, the P_{Tet} promoter was replaced with a $P_{lac/ara}$ promoter (Lutz and Bujard, 1997) using the *AatII* and *EcoR1* restriction sites. The plac/araL13YFP plasmids contain a $P_{lac/ara}$ promoter that regulates the expression of ribosomal protein L13 fused in frame with a C-terminal yellow fluorescent protein (YFP). An overnight culture of BL21Pro cells carrying the plac/araL13YFP was diluted 1000-fold into fresh LB (supplemented with 50µg/mL ampicillin) and grown overnight at 37^{o}C and 250 RPM. This culture was then washed three times in PBS, diluted 50X into 7mL of fresh M9 medium supplemented with 1mM IPTG and 0.1% arabinose and was incubated for 3 hours at 37^{o}C and 250 rotations per minute. Next, the culture was spun down, washed once with PBS, and resuspended into 7mL of fresh M9 medium. This culture was supplemented with either kanamycin (10µg/ml) or chloramphenicol (2µg/ml). 200µl of this culture was placed in a microplate and overlayed with 50µl mineral oil. The cultures were incubated in plate reader at 37^{o}C or 42^{o}C (to induce HSR). OD_{600} and YFP intensity were recorded at 10 minute intervals. Based on a 95% confidence level, the exponents of the fitted curves are significantly different

between kanamycin and chloramphenicol. Similarly chloramphenicol and chloramphenicol with heat shock are significantly different. L13-YFP profiles are significantly different between kanamycin and chloramphenicol (p-value=0.0029), chloramphenicol and heat shock and chloramphenicol (p-value=0.0029), and heat shock and chloramphenicol (p-value=0.0027). Finally, we performed additional model derivation (results not shown) by assuming a Michaelis-Menten degradation kinetic (by modifying the term "k_d[CA] to k_d[CA]/(K+[CA]) in Eq. S4 in Supplementary Materials). The final equation has the same structure as Eq. S13, which suggests that the model maintains its ability to generate bistability. Therefore, either the first-order or the Michaelis-Menten degradation dynamic gives rise to similar qualitative conclusion with regards to the generation of IE. We note that similar trends were observed at 1X, ~0.8X and 0.5X MIC (results not shown).

Ribosome purification (Supplementary Figure S1D)

To confirm that our L13-YFP fusion protein was associated with the ribosome, we purified crude ribosomes as previously described (Moore et al., 2008). BL21pro harboring plac/araL13YFP (p15a, Amp) or a plac/araYFP (p15a, Amp) plasmid (control) were grown overnight in 25mL LB medium supplemented with 50ug/mL ampicillin. The following day, 25mL of culture was diluted in 500mL of LB medium containing ampicillin and shaken for 1 hr at 37C (250 RPM). 1mM IPTG and 0.1% arabinose was then added to the medium and the cultures were shaken for 2 hrs. After 2 hrs, we confirmed expression of both L13YFP and YFP by detecting YPF signal in a microplate reader. Cultures were then cooled on ice, cells were isolated via centrifugation and washed once in wash buffer (40mM K^+HEPES pH 7.4, 100mM NaCl, 6.1mM Mg-OAc). Cells were then lysed for 30 min at room temperature in lysis buffer

(100mM K^+glutamate, 20mM HEPES Tris (pH 7.5), 0.1mM EDTA, 6.1mM Mg-OAC, 14mM β-mercaptoethanol, 0.05% Tween 20, 0.5mM $CaCl_2$, 1mg/mL lysozyme (from chicken egg white, Sigma Aldrich, St. Louis, MO), 1X DNase buffer (Carlsbad, CA, Invitrogen), 20 U of RNase-Free DNase (Invitrogen)). Cell lysate was precleared of cell debris by centrifuging the lysate four times at 4^{o}C for 10 minutes at 13,000 x g. The cleared lysate was then loaded on a 34mL 10% sucrose buffer (100mM K^+glutamate, 20mM HEPES Tris (pH 7.5), 0.1mM EDTA, 6.1mM Mg-OAC, 14mM β-mercaptoethanol, 0.05% Tween 20, 10% sucrose (RNase free, Sigma Aldrich). Ribosomes were pelletted at 26,000RPM for 19 hrs in an SW-28 rotor (Beckman Coulter Inc). The sucrose buffer was carefully removed and the pellet was resuspended in HT-6 buffer (100mM K^+glutamate, 20mM HEPES Tris (pH 7.5), 0.1mM EDTA, 6.1mM Mg-OAC, 14mM β-mercaptoethanol, 0.05% Tween 20). Following two additional centrifugation steps (10 minutes, 4^{o}C, 13,000 x g) to remove any remaining insoluble material, Abs260 (i.e., total RNA) was quantified using a Nanodrop (Thermo Fisher, Wilmington, DE). To detect the presence of YFP in the ribosomal pellet, YFP signal was quantified in a microplate. We note that in two experiments YFP signal in ribosomes isolated from cells containing the L13-YFP construct was ~500 fold higher than cells harboring p(lac/ara)EYFP (Supplementary Figure S1D). This large difference in signal intensity suggested that our fusion protein is integrated into the ribosomes. We note that nonspecific or transient interactions, as well as contaminating proteins that may fluoresce similar to YFP, would result in identical background signals from ribosomes isolated from both p(lac/ara)L13YFP and p(lac/ara)YFP containing cells.

rRNA extraction and measurement (Supplementary Figure S1E and H)

To assess rRNA amounts, we grew BL21 cells over night in 3mL LB medium at 37^{o}C (250RPM). The following day, the cells were diluted 50X into 40mL of M9 pre warmed (at 37^{o}C) medium and incubated them without shaking in a 37^{o}C waterbath until Abs600 was ~0.140. The culture was then split into 7mL fractions that were placed into separate 15mL tubes. At this time (t = 0), kanamycin (100μg/mL) or chloramphenicol (10μg/mL or 0.7μg/mL) was added and the tubes were incubated in the 37^{o}C waterbath. To validate if total rRNA increased in growing cultures, we also used an untreated culture. To allow a fair comparison between antibiotic treatments, these concentrations of antibiotics (kanamycin (100μg/mL) and chloramphenicol (10μg/mL)) were chosen as they resulted in nearly identical growth between kanamycin and chloramphenicol. We note that 0.7μg/mL of chloramphenicol was chosen as it lies within the IE region crated by exogenously applied heat shock (at 42^{o}C). To explore the effect of heat shock on rRNA, one culture was not treated with antibiotics but was instead incubated in at 42^{o}C waterbath while a second culture was treated with 1μg/ml and incubated at 42^{o}C. At *t = 0* and every hour thereafter for three hours, total RNA was isolated (two technical replicate extractions per data point) and Abs600 was measured (two technical replicates measurements per data point). Briefly. 500μl of culture was removed, spun at 21,000xg in a centrifuge for 2 minutes, the supernatant was removed and the cell pellet was frozen at -80^{o}C. For RNA extraction, 100μl of TE buffer (pH 8.0) containing 1mg/mL lysozyme (Sigma Aldrich) was added to the frozen pellet. This mixture was vortexed for 10 seconds and was then incubated on a rocker platform for 15 minutes. Total RNA was then extracted using an RNeasy minicolumn according to the manufacturer's instructions. Note that we performed the optional in column DNase digestion to

remove contaminating genomic DNA. Total RNA was quantified at Abs260 using a Nanodrop. We note that total RNA can be used as a metric for rRNA because only ~2% of total RNA is attributed to mRNA (Piir et al., 2011) and tRNA is removed by our RNA extraction method according to the manufacturer. Based on 95% confidence level (the same statistical analysis as in Supplementary Figure S1B), we observed that treatment with kanamycin or heat shock resulted in faster degradation of rRNA when compared to chloramphenicol (Supplementary Figure S1E, p-value<0.05). Furthermore, in growing cultures, the total amount of rRNA increased (Supplementary Figure S1H).

We note that chloramphenicol treatment (without heat shock) caused slight increase in the rRNA level. This is due to slight upregulation of ribosomal promoter by translation-inhibition antibiotics (Bollenbach et al., 2009). To ensure that the results observed in our rRNA degradation analysis were not due to differences in rRNA expression levels, we used a reporter plasmid (Amp, SC101) that contained the ribosomal promoter *rrnb* driving the expression of a green fluorescent protein (GFP). As such, GFP intensity can be used to measure *rrnB* activity. The plasmid used was constructed in a previous study (Zaslaver et al., 2006), but we changed the resistance marker from kanamycin to ampicillin. This plasmid was transformed into *E. coli* strain BL21. We grew two clones overnight in 3mL of liquid LB containing 50μg/mL ampicillin. We then diluted, grew (without ampicillin) and applied antibiotics (100μg/ml of kanamycin or 10μg/ml of chloramphenicol) to these cultures as described directly above. We then placed 200μl of each antibiotic treated culture in a 96 well plate (at 37^{o}C), overlayed each sample with 50μl of mineral oil and measured cell density (Abs600) and GFP intensity (a.u.) every 10 minutes. We observed that both kanamycin-treated and chloramphenicol-treated cultures had the same amount

of GFP signal normalized by cell density (Supplementary Figure S1F). The results suggest that the *rrnB* promoter activity was similar upon treatment by kanamycin or chloramphenicol.

Finally, as our *rrnb*-GFP reporter would be affected by translational inhibition due to the application of antibiotics, we wanted to ensure that the concentrations of kanamycin (100μg/ml) and chloramphenicol (10μg/ml) inhibited translation equally. Therefore, we grew *E. coli* strain BL21pro containing an anhydrotetracycline (atc) inducible P_{tet} promoter (Lutz and Bujard, 1997) driving the expression of a cyan fluorescent protein (CFP, p15a, Amp) and applied antibiotics as described above. After the application of antibiotics, we added a saturating amount (Lutz and Bujard, 1997) of atc, placed 200μl of each culture in a 96well plate (at 37^{o}C), covered each culture with 50μl of mineral oil, and measured CFP intensity every 10 minutes. Treatment with kanamycin or chloramphenicol resulted in identical levels of translational inhibition as determined by identical levels of CFP. We note that the levels of CFP produced under these antibiotics treatments were significantly less than those observed when cells were induced with atc but were not treated with antibiotics. These results are presented in Supplementary Figure S1G. Finally we note that differences in protein stability do not account for the similarity in *rrnB*-GFP results as treatment with chloramphenicol and kanamycin resulted in similar degradation rates of CFP (without an ssrA-tag, Supplementary Figure S1B).

Assessment of spontaneous mutants (Supplementary Figure S2D)

Spontaneous mutation cannot account for IE. This was assessed in two different experiments and through modeling. We diluted bacteria 50X in M9 medium and treated them with 10, 8 or 6 μg/ml of kanamycin until each culture began growing (i.e., when cultures with an OD_{600} of ~0.05 reached an OD_{600} of ~ 0.1). We note that these concentrations of kanamycin are

in the IE region. Next, we isolated single colonies from these cultures by diluting and plating the culture on LB agar medium (no antibiotics). Individual colonies were grown in liquid medium as described above (Strains, growth conditions, and medium) in the presence of kanamycin. As a control, we also grew BL21 that had not been previously exposed to antibiotics. We found that all colonies (12 total, 4 from each concentration of kanamycin (i.e., 10, 8 or 6 μg/ml) had the same of lower MIC as BL21 control cultures. As such, rapid generation of large quantities of spontaneous mutants do not account for growth in IE (Supplementary Figure S2D).

In another experiment, we grew and incubated BL21 as described above (Strains, growth conditions, and medium) in 10μg/ml kanamycin for 24 hours in M9 medium. Next, we isolated single colonies from these cultures by diluting and plating each culture on LB agar medium without antibiotics. 15 colonies were selected and grown in liquid medium as described above. We examined the kanamycin MIC of these isolated colonies relative to BL21 that was not previously grown in the presence on antibiotics and found that only 3 colonies had higher MIC levels that the BL21 control (Supplementary Figure S2D).

To corroborate these results, we formulated a simple model that accounts for mutant generation by a rate constant k_{mut} (resistant mutant/cell/min). We chose a range of rate constants k_{kill} (min^{-1}) where an antibiotic completely inhibits growth of sensitive bacteria. The simulation results suggest that only very high mutation rate constants ($>10^{-2}$/cell/min) can generate observable growth of a population due to mutation (Supplementary Figure S2E). Such mutation rates are much higher than the observed mutation rates in the literature ($\sim10^{-9}$/cell/min) (Kohanski et al., 2010). Therefore, both our experimental and modeling data suggests that spontaneous mutation cannot account for IE.

Testing for a communication-based resistance (Supplementary Figure S2F and S2G)

First, to test contribution by quorum sensing or enzyme/molecule secretion, we grew BL21 cells in the spent medium derived from BL21 cultures challenged with varying concentrations of kanamycin. We diluted BL21 50X as described above (Strains, growth conditions, and medium) and grew this culture for 6 hours in 0, 6, 8 10, and 12μg/mL of kanamycin. The spent media from these cultures were then filtered using a 0.2μm cellulose acetate filter (VWR, Radnor, PA) and stored at -20^{o}C overnight. The following day, an overnight culture of BL21 was diluted 500X into both the spent media and a fresh medium. The spent media did not rescue bacteria from kanamycin treatment as populations grown in either the spent media or a fresh medium had the same MIC of kanamycin (Supplementary Figure S2F). If a quorum sensing based system (i.e., activation of a cellular pathway above a critical cell density) were responsible for IE, then one would expect the 500X dilution to grow at the same concentrations as the 50X dilution in the spent medium. These results indicate that extracellular communication factors or secreted components are not the cause of IE in our experiments.

Second, to specifically rule out an indole based resistance mechanism, we tested a *tnaA* (which creates indole, the molecule responsible for the resistance mechanism described in (Lee et al., 2010b)) knockout mutant (strain BW25113) (Baba et al., 2006) for IE using streptomycin as described above (Strains, growth conditions, and medium). We note that this mutant strain exhibited IE (Supplementary Figure S2G), which suggests that indole secretion does not play a major role in generating IE.

Antibiotic susceptibility tests

We conducted two tests to verify the growth dynamics (Figure 2A). First, bacteria might have gained resistance to kanamycin by adaptive mutation. To test this possibility, we stored stationary cultures from the experiments (Figure 2A, 10μg/ml) as a glycerol stock. Next, we prepared overnight cultures by using the glycerol stock. The overnight cultures were then diluted 1000-fold into fresh M9 medium supplemented with either 10μg/ml or 50μg/ml kanamycin. We observed no bacterial growth in the medium, indicating that these bacteria had not acquired spontaneous resistance to kanamycin.

Second, kanamycin might be unstable in M9 medium resulting in rapid decay of the antibiotic and a subsequent decrease of antibiotic concentration. To rule out this possibility, we incubated kanamycin in M9 medium at 37^{o}C for 6 hours. Bacteria inoculated into this medium displayed similar growth dynamics (results not shown). Therefore, the observed dynamics were not due to the decay of kanamycin.

Flow system (Figure 5A)

All components of the flow system were purchased from Harvard Apparatus (Massachusetts, USA). A computer controlled the flow valves in order to select the source of medium. Flow rate was regulated by the flow rate controller. The minimum height difference between the medium reservoirs and the cell chamber was 3cm, which allowed for a maximum flow rate of approximately 2ml/minute. The flow rate used in all experiments was approximately 0.2ml/minute. We used a cell chamber (Ibidi, Martinsried, Germany) made of uncoated hydrophobic glass to allow bacterial adherence to the bottom. Bacteria were imaged by using an

inverted microscope (Leica, IL, USA) using a 100X objective. For each experiment, phase contrast images of five fields were recorded at 10 minute intervals for at least eight hours. The number of bacteria in each image was enumerated by using the CellC program(Selinummi et al., 2005). We note that the enumeration was less accurate at high bacterial density due to limitation in the segmentation algorithm. Red fluorescence was recorded by using a mercury excitation lamp, a 546±6nm excitation filter, and a 605±37.5nm emission filter.

To measure the response time of the flow system, we used dH_2O as medium 1 and dH_2O containing the red fluorescent dye sulforhodamine as medium 2. Supplementary Figure S5B shows the average fluorescence of one field with a pulse period of 40 minutes. Sulforhodamine reached equilibrium rapidly, which closely matched the input square wave pattern.

Specifically, we incubated bacteria using medium supplemented with either 10μg/ml kanamycin (that caused IE) or 10μg/ml chloramphenicol (that did not cause IE). After treatment for a specific duration, we washed bacteria using fresh medium and then tracked population growth. We quantified recovery time as the time required for a population to increase above its initial density after antibiotic treatment.

Bacterial response to pulsatile antibiotic treatment (Figure 5C, Figure 7, Supplementary Figure S5C&D ,and Figure S7)

Overnight cultures were diluted 1000-fold into 10ml fresh M9 medium. The cultures were shaken for one hour at 37^{o}C and at 250 rotations per minute. In order for bacteria to adhere to the bottom of the chamber, the cultures were added to the cell chamber and incubated without medium flow for 15 minutes at 37^{o}C. For studies of recovery time, cells were exposed to a single

pulse of antibiotic. Otherwise, cells were exposed to different periods of antibiotics by alternating the medium in the cell chamber. To completely replace a medium in the cell chamber, the flow valve of the other medium reservoir was opened for two minutes before closing. We note that two minutes was longer than the response time of the system (Supplementary Figure S5B) and was therefore sufficient to replace the medium in the cell chamber.

As recommended by the manufacturer of our microscope, we performed the 42^{o}C pulse experiments (Fig. S7D) in a forced-air incubator that was housed separately from the microscope. As such, we were not able to acquire images of the initial bacterial density attached to each chamber for this experiment. Initial bacterial densities were controlled tightly by using the same preparation steps as in Figure 7. In addition, we observed consistent results in experiments performed on different days. Finally, we note that some images in Figure S7D were taken using a Zeiss Axiovert 200M microscope using identical magnification settings as in Figure 7 and Figure S7C.

SUPPLEMENTARY RESULTS

Model development, justification, and simplification

We modeled the inhibition of bacterial growth by antibiotics by using the following equations (Equations S1-S5).

$$\frac{d[C]}{dt} = k_0 + \frac{k_1[C]}{V_1 + [C]} - k_u[C] - k_f[C][A]_{in} + k_b[CA] \qquad [S1]$$

$$\frac{d[A]_{in}}{dt} = k_{in}[A]_{out} - k_{out}[A]_{in} - k_f[C][A]_{in} + k_b[CA] + k_r[CA'] \quad [S2]$$

$$\frac{d[A]_{out}}{dt} = -(k_{in}[A]_{out} - k_{out}[A]_{in})\frac{V_c N}{V_m} \quad [S3]$$

$$\frac{d[CA]}{dt} = k_f[C][A]_{in} - k_b[CA] - k_d[CA] \quad [S4]$$

$$\frac{d[CA']}{dt} = k_d[CA] - k_r[CA'] \quad [S5]$$

where C represents the core component (nM), A_{in} represents the intracellular antibiotic concentration (nM), A_{out} represents the extracellular antibiotic concentration (nM), CA represents complex of C and A_{in} (nM), CA' represent degradation product of CA (nM), k_0 represents the leaky synthesis rate constant of C (nM min^{-1}), k_1 represents the synthesis rate constant of C (nM min^{-1}), V_1 represents C at half k_1 (nM), k_u represents both the degradation rate constant and utilization rate constant of C (min^{-1}), k_f represents binding rate constant of A_{in} to C (nM^{-1} min^{-1}), k_b represents dissociation rate of the AC complex (min^{-1}), k_{in} represents the influx of antibiotics into bacteria (min^{-1}), and k_{out} represents the efflux of antibiotics into bacteria (min^{-1}). For simplicity, we have assumed that the leaky synthesis term k_0 is a constant term, instead of being proportional to ribosome levels as its magnitude is likely small relative to other terms in the equation. We note that with or without the leaky synthesis term, the qualitative aspects of the model remain unchanged.

Here, we modeled the multi-step degradation of CA (e.g., ribosome-antibiotic complex(Edmunds and Goldberg, 1986; Kaplan and Apirion, 1975)) by using the intermediate

complex *CA'*. Therefore, k_d represents the initial targeting of *CA* by proteases and ribonucleases, after which *CA* could not be reversed to allow free and functional *C*. This assumption is consistent with the observation that non-translating ribosomes are the major targets of degradation(Zundel et al., 2009). Since an increased k_d effectively increases the degradation rate of *CA*, we referred to k_d (min^{-1}) as the antibiotic-induced degradation of proteins in the main text. Along this line, k_r (min^{-1}) represents the release of *A* throughout the multi-step degradation. Previous studies have shown that certain antibiotics, such as kanamycin and streptomycin, but not antibiotics, such as tetracycline and chloramphenicol, elicit the heat shock response (HSR) when proteins become mistranslated/misfolded (Goff and Goldberg, 1985; Parsell and Sauer, 1989; Pinkett and Brownstein, 1974). This, in turn, leads to increased protease activity (Goff et al., 1984; Lindquist, 1986; Parsell and Lindquist, 1993). Furthermore, it has been demonstrated that increased protease activity occurs after treatment with aminoglycosides (Marr et al., 2007). In addition, heat shock, as well as treatment with antibiotics such as streptomycin, but not chloramphenicol, also been shown to cause increased degradation of rRNA(Deutscher, 2003; Dubin, 1964; Nozawa et al., 1967; Rosenthal and Iandolo, 1970; Suzuki and Kilgore, 1967; Tolker-Nielsen and Molin, 1996). To support our model and corroborate previous findings, we first demonstrated that certain antibiotics lead to HSR (Supplementary Figure S1A). Next, we showed that proteins specifically targeted to the ClpXP (Gottesman et al., 1998) and lon (Choy et al., 2007) proteases (i.e., an SsrA-tagged CFP) were degraded faster when cells were treated with antibiotics that result in HSR (Supplementary Figure S1B). Finally, we demonstrated that the ribosomal protein L13 (fused to a YFP reporter) was degraded faster in response to antibiotics that cause HSR than antibiotics that did not cause HSR (Supplementary Figure S1C). We note that this ribosomal protein has been previously shown to be degraded by the Lon protease during

cellular stress(Kuroda et al., 2001). In addition, we have demonstrated that rRNA is degraded faster when cells are treated with kanamycin or heat shock at 42^{o}C than when they are treated with chloramphenicol (Supplementary Figure S1E).

We note that HSR also increases the expression of chaperones, which assist with proper protein folding (Lindquist, 1986; Neidhardt et al., 1984). As higher protein stability could increase microbial survival rates in the presence of drug (Cowen and Lindquist, 2005), this response is unlikely to contribute to generation of IE as its effect would be independent of cell density (Figure 2A).

To simplify the model, we assume that the complex *CA*, A_{out}, and the complex *CA'* are in quasi-steady state.

$$[CA] = \frac{k_f [C][A]_{in}}{k_b + k_d} \qquad [S6]$$

$$[A]_{out} = \frac{k_{out}[A]_{in}}{k_{in}} \qquad [S7]$$

$$[CA'] = \frac{k_d [CA]}{k_r} \qquad [S8]$$

Next, we applied mass conservation of the antibiotic:

$$[A]_{in} V_c N + [A]_{out} V_m + [CA] V_c N + [CA'] V_c N = [A]_T V_m \qquad [S9]$$

where V_m represents the volume of medium (2x10^{-4}L in our experiment), V_c represents the bacterium volume (10^{-15}L per bacterium), and *N* represent the number of bacterium.

We substituted Equations S6-S8 into Equation S9.

$$[A]_{in}V_cN + \frac{k_{out}[A]_{in}}{k_{in}}V_m + (1+\frac{k_d}{k_r})\frac{k_f[C][A]_{in}}{k_b+k_d}V_cN = [A]_T V_m$$

$$\Rightarrow [A]_{in} = \frac{[A]_T}{\frac{V_cN}{V_m} + \frac{k_{out}}{k_{in}} + (1+\frac{k_d}{k_r})\frac{k_f[C]}{k_b+k_d}\frac{V_cN}{V_m}} \quad \text{[S10]}$$

We substituted Equations S6 and S10 into Equation S1 to obtain Equation S11.

$$\frac{d[C]}{dt} = k_0 + \frac{k_1[C]}{V_1+[C]} - k_u[C] - \frac{[A]_T[C]}{\frac{k_b+k_d}{k_dk_f}(\frac{V_cN}{V_m}+\frac{k_{out}}{k_{in}}) + \frac{1}{k_d}(1+\frac{k_d}{k_r})\frac{V_cN}{V_m}[C]} \quad \text{[S11]}$$

To simplify the equation, we note that $\frac{V_cN}{V_m} << \frac{k_{out}}{k_{in}}$ (bacterial volume is typically much smaller than culture volume). If $\frac{k_d}{k_r} >> 1$, initial targeting of degradation is faster than multi-step degradation. Equation S11 was transformed to Equation S12.

$$\frac{d[C]}{dt} = k_0 + \frac{k_1[C]}{V_1+[C]} - k_u[C] - \frac{[A]_T k_r[C]}{\frac{k_b+k_d}{k_f}\frac{k_{out}}{k_{in}}\frac{k_r}{k_d} + \frac{V_cN}{V_m}[C]} \quad \text{[S12]}$$

Next, we non-dimensionalized Equation S12 to obtain Equation S13.

$$\frac{dc}{d\tau} = \alpha + \frac{c}{\kappa + c} - (1 + \frac{\phi}{\delta + \gamma c})c \qquad [S13]$$

where $c = \frac{k_u}{k_1}[C]$, $\tau = k_u t$, $\alpha = \frac{k_0}{k_1}$, $\kappa = \frac{V_1 k_u}{k_1}$, $\phi = \frac{[A]_T k_r}{k_1}$, $\gamma = \frac{V_c N}{V_m}$, and $\delta = \frac{(k_b + k_d)}{k_f}\frac{k_{out}}{k_{in}}\frac{k_r}{k_d}\frac{k_u}{k_1}$.

δ increases with decreasing k_d, increasing k_b, and increasing k_{out}. Based on Equation S13, the initial bacterial density N would affect the parameter γ and antibiotic-induced degradation would affect the parameter δ.

On the other hand, if $\frac{k_d}{k_r} << 1$, degradation is negligible. Equation S11 was transformed to Equation S14.

$$\frac{d[C]}{dt} = k_0 + \frac{k_1[C]}{V_1 + [C]} - k_u[C] - \frac{k_d[A]_T[C]}{\frac{k_b + k_d}{k_f}\frac{k_{out}}{k_{in}} + \frac{V_c N}{V_m}[C]} \qquad [S14]$$

Since $\frac{k_d}{k_r} << 1$, we could assume that $k_d << k_b$. Furthermore, without antibiotic-induced degradation, the magnitude of $\frac{k_b + k_d}{k_f}\frac{k_{out}}{k_{in}} >> \frac{V_c N}{V_m}[C]$. Thus, Equation S14 was transformed to Equation S15.

$$\frac{d[C]}{dt} = k_0 + \frac{k_1[C]}{V_1 + [C]} - k_u[C] - \frac{k_d[A]_T[C]}{\frac{k_b}{k_f}\frac{k_{out}}{k_{in}}} \qquad [S15]$$

Equation S15 cannot generate bistability, which is qualitatively similar to the case when k_d is small in Equation S13. Therefore, we only presented Equation S13 in the main text.

To model population growth (Figure 5A and B), we added Equation S16 to Equations S1-S5:

$$\frac{dN}{dt} = \varphi\frac{[C]}{V + [C]}N(1 - \frac{N}{N_{\max}}) \qquad [S16]$$

where N represents the bacterial density, N_{max} (=10^9) represents the carrying capacity of a medium, ϕ (=0.02 min^{-1}) represents the growth rates, and V (=0.1) represents the C level that gives the half maximal growth rates. Equation S16 is inspired by the dependence of growth rates on the number of ribosomes in bacteria(Neidhardt, 1996). Specifically, growth rates increase with increasing ribosomes, but saturate at a ribosome level. We note the use of an alternative

growth equation, such as that in (Fange et al., 2009), would not impact the qualitative predictions of our model.

Models that include the up-regulation of ribosomal promoters

Both the literature and our data demonstrated that ribosomal promoters are up-regulated during antibiotic treatment. To investigate the impact of such up-regulation on the bistability of the system, we included an additional term in the 2nd term of Eq. 1 to model the increase in synthesis rates of *C* (Equation S17). Here, we assumed that the up-regulation is dependent on levels of antibiotic inhibition, which is represented by [*CA*]. Furthermore, we assumed that the up-regulation could increase [*C*].

$$\frac{d[C]}{dt} = k_0 + \frac{k_1[C]}{V_1+[C]} \times \frac{k_2[CA]}{V_2+[CA]} - k_u[C] - \frac{[A]_T k_r[C]}{\frac{k_b+k_d}{k_f}\frac{k_{out}}{k_{in}}\frac{k_r}{k_d} + \frac{V_c N}{V_m}[C]} \quad \text{[S17]}$$

Following similar simplification steps as above, we obtained Equation S18 for a high k_d (based on Equation S12):

$$\frac{d[C]}{dt} = k_0 + \frac{k_1[C]}{V_1+[C]} \times \frac{k_2[A]_T[C]}{V_2\frac{k_b+k_d}{k_f}\frac{k_{out}}{k_{in}} + \frac{k_d}{k_r}\frac{V_c N}{V_m}[C] + [A]_T[C]} - k_u[C] - \frac{[A]_T k_r[C]}{\frac{k_b+k_d}{k_f}\frac{k_{out}}{k_{in}}\frac{k_r}{k_d} + \frac{V_c N}{V_m}[C]} \quad \text{[S18]}$$

Here, the synthesis term (2nd term) has a higher Hill's coefficient due to a new multiplier term, which models the up-regulation of *rrn* promoters. As such, the system is more likely to generate bistablity (nullcline analysis not shown). Hence, the up-regulation of *rrn* promoters by kanamycin would further enhance the generation of IE due to the enhanced degradation.

For comparison, we also obtained Equation S19 for a low k_d (based on Equation S15):

$$\frac{d[C]}{dt} = k_0 + \frac{k_1[C]}{V_1 + [C]} \times k_2 - k_u[C] - \frac{k_d[A]_T[C]}{\frac{k_b}{k_f}\frac{k_{out}}{k_{in}}} \quad \text{[S19]}$$

Here, the multiplier term could be reduced to a single term k_2 due to a low value of k_d. As such, the system is less likely to generate bistability (nullcline analysis not shown). Therefore, even though chloramphenicol up-regulates the *rrn* promoters, it could not generate IE.

Discussion of alternative hypothesis

To date, there have been several previously mechanisms of bacterial tolerance. In order to rule out previously described mechanisms, we summarize either modeling, experimental or literature evidence that strongly supports our claim that IE is generated when an antibiotic causes heat shock and results in ribosome degradation. See Supplemental Methods (above) for further details on the experimental analysis.

Supplementary Table S2: Alternative mechanisms that were ruled out by experimental or modeling results

Category	Specific mechanism	Counter argument			Note
		Model (this study)	Experiment (this study)	Literature	
Concentration	Titration of antibiotic by bacteria	O	O	O	A
Mutation	Resistance to antibiotic	O	O	O	B
Cell-cell communication	Outer membrane vesicles		O	O	C
	Quorum sensing		O	O	D
	Death factor			O	E
	Indole		O	O	F
	Antibiotic-degrading enzyme		O	O	G
	Secretion of H_2S		O	O	H
Molecular property of antibiotic	Binding sites, binding affinity and reversibility, transport, solubility, cooperativity, inhibition mode		O		I
Intracellular pathways	Persister	O	O	O	J
Metabolic State	Differences in initial metabolic states and adaptive response could underlie IE.		O	O	K

A. We note that our experimental results cannot be explained by the ratio of antibiotic molecules to the number of bacteria. We formulated a simple model that accounts for only the titration of antibiotics by a bacteria population. However, this model *always* gives rise to IE (results not shown), which is opposite of both our observation (Figure 2B) and literature data (Brook, 1989).

$$\frac{dN}{dt} = \mu N(1 - \frac{N}{Nm}) - kNA$$

$$\frac{dA}{dt} = -kNA$$

where N represents the bacterial density, Nm represents the carrying capacity, k represents the titration of antibiotics by bacteria, and A represents the antibiotic.

B. We formulated a simple model that accounts for mutant generation by a rate constant k_{mut} (resistant mutant/cell/min). We chose a range of rate constants k_{kill} (min^{-1}) where an antibiotic completely inhibits bacterial growth. The simulation results suggest that only very high mutation rate constants (>0.01 resistant mutant /cell/min) would generate observable growth of a population (Supplementary Figure S2E). Such mutation rates are higher than the observed mutation rates in the literature (~10^{-9}/cell/min)(Kohanski et al., 2010). Furthermore, our experiments (see above, SI) demonstrated that spontaneous mutants do not account for IE.

C. To examine the contribution of extracellular factors to the inoculum effect, we isolated spent media of bacterial cultures grown in 0, 6, 8 10, or 12μg/ml kanamycin (Supplementary Figure S2F). *E. coli* BL21 cells grown in both the spent media and a fresh medium had the same MIC. This result indicates that the spent media did not contain factors that could substantially rescue bacteria from kanamycin treatment. As such, this experimental result ruled out the contribution of cell-cell communication to IE (C-G).

D. Quorum-sensing based pathways are unlikely the causes of IE because BL21 does not have the AI-2 quorum sensing pathways based on recent sequencing results(Studier et al., 2009). We

also note that quorum-sensing factors have been ruled out due to the experiments performed (Supplementary Figure S2F) and our explanation in C.

E. Previous studies have indicated that higher concentrations of cells may be more susceptible to antibiotic treatment (Kolodkin-Gal et al., 2007; Kolodkin-Gal et al., 2008), which is opposite of IE. This behavior has been linked to the secretion of extracellular death factor (EDF), where a higher concentration of EDF increases the killing of bacteria by antibiotics. We note that the *E. coli* strain in this study appears to lack *ygeO* (Studier et al., 2009), which is a gene required for EDF production.

F. Recently, indole secretion has been implicated in antibiotic resistance (Lee et al., 2010a). However, this study has implicated mutation as the cause of constant indole production that leads to antibiotic resistance. Furthermore, without mutation, indole is not produced by bacteria under antibiotic stress. As such, this mechanism is highly unlikely to account for IE as a mutation leading to constitutive indole secretion would have to occur at very high frequency in our experiments. Furthermore, we tested the growth of BW25113 cells with a *tnaA* knockout, which cannot produce indole. These cells exhibited IE with streptomycin (Supplementary Figure S2G), which suggests that indole production is not the mechanism underlying IE.

G. If an enzyme was degrading the antibiotics in this study, the enzyme would have to be able to degrade all the seven antibiotics from two different classes, aminoglycosides and aminonucleosides. Such broad resistance across antibiotic classes is unlikely to occur due to the high structural specificity of antibiotic degrading enzyme (Magnet and Blanchard, 2005; Mingeot-Leclercq et al., 1999). Furthermore, we note that if antibiotics were enzymatically degraded, this would result in high minimum inhibitory concentration (MIC) values. We note that the MIC values obtained in our studies are on par with previous studies (Bayer et al., 1985).

H. The secretion of H_2S was observed to confer antibiotic resistance to bacteria(Shatalin et al., 2011). We observed that *sseA* knockout strains (produces significantly less H2S) still exhibited IE (Supplementary Figure S2H).

I. We note that physical property of antibiotics is not the fundamental reason underlying IE because chloramphenicol coupled with heat shock generated IE (Figure 4C & Supplementary Figure S4E), but chloramphenicol alone did not generate IE. However, high influx rate constants and tight binding between antibiotics and their targets are necessary but insufficient conditions to generate IE.

J. Persister cells could hypothetically generate IE by two ways:

1) They form at extremely *high* frequency (10^{2}/min) and grow at normal rates *during* antibiotic treatment (based on modeling prediction). As such, they account for all the observed growth in our IE experiments.
2) They stay dormant, but uptake a significant amount of antibiotics to promote the growth of normal bacteria.

These hypothetical mechanisms, however, contradict with both literature and our observation. First, previous studies have shown that persisters form at extremely low frequency ($<10^{-8}$/min(Balaban et al., 2004)). Second, persisters are subpopulations of cells that stay dormant under antibiotic treatment and that are not killed by antibiotics. They are typically observed by tracking bacterial recovery *after* the removal of antibiotics (Balaban et al., 2004). Therefore, it is unlikely that persisters would grow during antibiotic treatment in our batch cultures. Furthermore, we did not observe any bacterial recovery for as long as 16 hours after the removal of antibiotics (Figure 7, kanamycin 480min treatment), which suggests that persisters did not form at high rates in our experiments. Third, it has been demonstrated that persisters (that stay dormant) resist aminoglycosides by reducing the uptake of antibiotics (Allison et al., 2011). Once potentiated by metabolite, persisters uptake more antibiotics and are killed by the antibiotics. This literature data suggests that persisters cannot stay dormant while uptaking large amount of antibiotics at the same time.

K. In a previously proposed mechanism of IE (Greenwood, 1976), it was suggested that differences in initial metabolic state could create subpopulations of cells resistant to antibiotics and that such populations could emerge in the early growing stage. However, in contrast to this previous study, the cells in our manuscript have the same initial metabolic state. Furthermore, we have quantitatively studied the emergence timing of resistant bacteria in our mutation analysis (Supplementary Figure S2D), which demonstrates that resistant sub populations cannot account for the initial emergence of growth in our system. However, given the presence of colonies with high MIC at later stages of growth (i.e., 24 hours), it is possible that a resistant sub population could emerge during later stages of growth as a result of IE.

Finally, we note that we have ruled out the potential contribution of technical factors in our experimental technique. Washing the cells from overnight cultures in PBS prior to dilution in fresh M9 medium did not fundamentally impact the occurrence of IE with kanamycin (not shown). Furthermore, previous studies have indicated that reductions in pH can decrease aminoglycoside activity(Gudmundsson et al., 1991). To rule out pH changes as the mechanism of IE, we buffered the medium to pH 7.5. Indeed, bacteria grown in buffered medium continued to show IE with kanamycin (not shown).

Supplementary Table S3: List of plasmids used in this study

Plasmid Name	Construct of Interest	Promoter	Replication Origin	Resistance Marker
p(lac/ara)L13YFP	Fusion between r*plM* (L13) and EYFP	$P_{lac/ara}$*	p15a	Ampicillin
p(lac/ara)YFP	EYFP	$P_{lac/ara}$*	p15a	Ampicillin
rrnB-GFP	Ribosomal rRNA promoter rrnB driving GFP	*rrnB*#	SC101	Ampicllin
pTetCFPlaa	CFP with an SsrA degradation tag	P_{Tet}*	p15a	Ampicillin
pTetCFP	CFP	P_{Tet}*	p15a	Ampicillin

*promoter from Lutz and Bujard, 1997, #from Zaslaver et al., 2006

SUPPLEMENTAL REFERENCES

Allison, K.R., Brynildsen, M.P., and Collins, J.J. (2011). Metabolite-enabled eradication of bacterial persisters by aminoglycosides. Nature *473*, 216-220.

Baba, T., Ara, T., Hasegawa, M., Takai, Y., Okumura, Y., Baba, M., Datsenko, K.A., Tomita, M., Wanner, B.L., and Mori, H. (2006). Construction of Escherichia coli K-12 in-frame, single-gene knockout mutants: the Keio collection. Mol Syst Biol *2*.

Balaban, N.Q., Merrin, J., Chait, R., Kowalik, L., and Leibler, S. (2004). Bacterial persistence as a phenotypic switch. Science *305*, 1622-1625.

Bayer, A.S., Norman, D., and Anderson, D. (1985). Efficacy of ciprofloxacin in experimental arthritis caused by Escherichia coli--in vitro-in vivo correlations. J Infect Dis *152*, 811-816.

Bollenbach, T., Quan, S., Chait, R., and Kishony, R. (2009). Nonoptimal microbial response to antibiotics underlies suppressive drug interactions. Cell *139*, 707-718.

Brook, I. (1989). Inoculum effect. Rev Infect Dis *11*, 361-368.

Choy, J.S., Aung, L.L., and Karzai, A.W. (2007). Lon Protease Degrades Transfer-Messenger RNA-Tagged Proteins. J Bacteriol *189*, 6564-6571.

Cowen, L.E., and Lindquist, S. (2005). Hsp90 potentiates the rapid evolution of new traits: drug resistance in diverse fungi. Science *309*, 2185-2189.

Deutscher, M.P. (2003). Degradation of stable RNA in bacteria. J Biol Chem *278*, 45041-45044.

Dubin, D.T. (1964). Some effects of streptomycin on RNA metabolism in Escherichia coli. Journal of Molecular Biology *8*, 749-767.

Edmunds, T., and Goldberg, A.L. (1986). Role of ATP hydrolysis in the degradation of proteins by protease La from Escherichia coli. J Cell Biochem *32*, 187-191.

Fange, D., Nilsson, K., Tenson, T., and Ehrenberg, M.n. (2009). Drug efflux pump deficiency and drug target resistance masking in growing bacteria. Proceedings of the National Academy of Sciences *106*, 8215-8220.

Goff, S.A., Casson, L.P., and Goldberg, A.L. (1984). Heat shock regulatory gene htpR influences rates of protein degradation and expression of the lon gene in Escherichia coli. Proc Natl Acad Sci U S A *81*, 6647-6651.

Goff, S.A., and Goldberg, A.L. (1985). Production of abnormal proteins in E. coli stimulates transcription of lon and other heat shock genes. Cell *41*, 587-595.

Gottesman, S., Roche, E., Zhou, Y., and Sauer, R.T. (1998). The ClpXP and ClpAP proteases degrade proteins with carboxy-terminal peptide tails added by the SsrA-tagging system. Genes & Development *12*, 1338-1347.
Greenwood, D. (1976). Differentiation of mechanisms responsible for inoculum effects in the response of Escherichia coli to a variety of antibiotics. Journal of Antimicrobial Chemotherapy *2*, 87-95.
Gudmundsson, A., Erlendsdottir, H., Gottfredsson, M., and Gudmundsson, S. (1991). Impact of pH and cationic supplementation on in vitro postantibiotic effect. Antimicrobial Agents and Chemotherapy *35*, 2617-2624.
Kaplan, R., and Apirion, D. (1975). The fate of ribosomes in Escherichia coli cells starved for a carbon source. J Biol Chem *250*, 1854-1863.
Kohanski, M.A., Depristo, M.A., and Collins, J.J. (2010). Sublethal antibiotic treatment leads to multidrug resistance via radical-induced mutagenesis. Mol Cell *37*, 311-320.
Kohanski, M.A., Dwyer, D.J., Wierzbowski, J., Cottarel, G., and Collins, J.J. (2008). Mistranslation of membrane proteins and two-component system activation trigger antibiotic-mediated cell death. Cell *135*, 679-690.
Kolodkin-Gal, I., Hazan, R., Gaathon, A., Carmeli, S., and Engelberg-Kulka, H. (2007). A linear pentapeptide is a quorum-sensing factor required for mazEF-mediated cell death in Escherichia coli. Science *318*, 652-655.
Kolodkin-Gal, I., Sat, B., Keshet, A., and Engelberg-Kulka, H. (2008). The communication factor EDF and the toxin-antitoxin module mazEF determine the mode of action of antibiotics. PLoS Biol *6*, e319.
Kuroda, A., Nomura, K., Ohtomo, R., Kato, J., Ikeda, T., Takiguchi, N., Ohtake, H., and Kornberg, A. (2001). Role of inorganic polyphosphate in promoting ribosomal protein degradation by the Lon protease in E. coli. Science *293*, 705-708.
Lee, H.H., Molla, M.N., Cantor, C.R., and Collins, J.J. (2010a). Bacterial charity work leads to population-wide resistance. Nature *467*, 82-85.
Lee, H.H., Molla, M.N., Cantor, C.R., and Collins, J.J. (2010b). Bacterial charity work leads to population-wide resistance. Nature *467*, 82-85.
Lindquist, S. (1986). The heat-shock response. Annu Rev Biochem *55*, 1151-1191.

Lutz, R., and Bujard, H. (1997). Independent and Tight Regulation of Transcriptional Units in Escherichia Coli Via the LacR/O, the TetR/O and AraC/I1-I2 Regulatory Elements. Nucleic Acids Research *25*, 1203-1210.
Magnet, S., and Blanchard, J.S. (2005). Molecular insights into aminoglycoside action and resistance. Chem Rev *105*, 477-498.
Marr, A.K., Overhage, J., Bains, M., and Hancock, R.E.W. (2007). The Lon protease of Pseudomonas aeruginosa is induced by aminoglycosides and is involved in biofilm formation and motility. Microbiology *153*, 474-482.
Mingeot-Leclercq, M.P., Glupczynski, Y., and Tulkens, P.M. (1999). Aminoglycosides: activity and resistance. Antimicrob Agents Chemother *43*, 727-737.
Moore, S.D., Baker, T.A., and Sauer, R.T. (2008). Forced extraction of targeted components from complex macromolecular assemblies. Proceedings of the National Academy of Sciences *105*, 11685-11690.
Neidhardt, F.C., ed. (1996). Escherichia Coli and Salmonella: Cellular and Molecular Biology (Washington DC, American Society Microbiology).
Neidhardt, F.C., VanBogelen, R.A., and Vaughn, V. (1984). The genetics and regulation of heat-shock proteins. Annu Rev Genet *18*, 295-329.
Nozawa, R., Horiuchi, T., and Mizuno, D. (1967). Degradation of ribosomal RNA in a temperature-sensitive Escherichia coli. Archives of Biochemistry and Biophysics *118*, 402-409.
Parsell, D.A., and Lindquist, S. (1993). The function of heat-shock proteins in stress tolerance: degradation and reactivation of damaged proteins. Annu Rev Genet *27*, 437-496.
Parsell, D.A., and Sauer, R.T. (1989). Induction of a heat shock-like response by unfolded protein in Escherichia coli: dependence on protein level not protein degradation. Genes & Development *3*, 1226-1232.
Pinkett, M.O., and Brownstein, B.L. (1974). Streptomycin-Induced Synthesis of Abnormal Protein in an Escherichia coli Mutant. Journal of Bacteriology *119*, 345-350.
Rosenthal, L.J., and Iandolo, J.J. (1970). Thermally Induced Intracellular Alteration of Ribosomal Ribonucleic Acid. J Bacteriol *103*, 833-835.

Selinummi, J., Seppala, J., Yli-Harja, O., and Puhakka, J.A. (2005). Software for quantification of labeled bacteria from digital microscope images by automated image analysis. Biotechniques *39*, 859-863.

Shatalin, K., Shatalina, E., Mironov, A., and Nudler, E. (2011). H2S: A Universal Defense Against Antibiotics in Bacteria. Science *334*, 986-990.

Studier, F.W., Daegelen, P., Lenski, R.E., Maslov, S., and Kim, J.F. (2009). Understanding the differences between genome sequences of Escherichia coli B strains REL606 and BL21(DE3) and comparison of the E. coli B and K-12 genomes. J Mol Biol *394*, 653-680.

Suzuki, H., and Kilgore, W.W. (1967). Decomposition of Ribosomal Particles in Escherichia coli treated with Mitomycin C. J Bacteriol *94*, 666-676.

Tan, C., Marguet, P., and You, L. (2009). Emergent bistability by a growth-modulating positive feedback circuit. Nat Chem Biol *5*, 842-848.

Tolker-Nielsen, T., and Molin, S. (1996). Role of ribosome degradation in the death of heat-stressed Salmonella typhimurium. FEMS Microbiology Letters *142*, 155-160.

Vanbogelen, R.A., and Neidhardt, F.C. (1990). Ribosomes as sensors of heat and cold shock in Escherichia-Coli. Proceedings of the National Academy of Sciences of the United States of America *87*, 5589-5593.

Zaslaver, A., Bren, A., Ronen, M., Itzkovitz, S., Kikoin, I., Shavit, S., Liebermeister, W., Surette, M.G., and Alon, U. (2006). A comprehensive library of fluorescent transcriptional reporters for Escherichia coli. Nat Meth *3*, 623-628.

Zundel, M.A., Basturea, G.N., and Deutscher, M.P. (2009). Initiation of ribosome degradation during starvation in Escherichia coli. RNA *15*, 977-983.

Figure S1

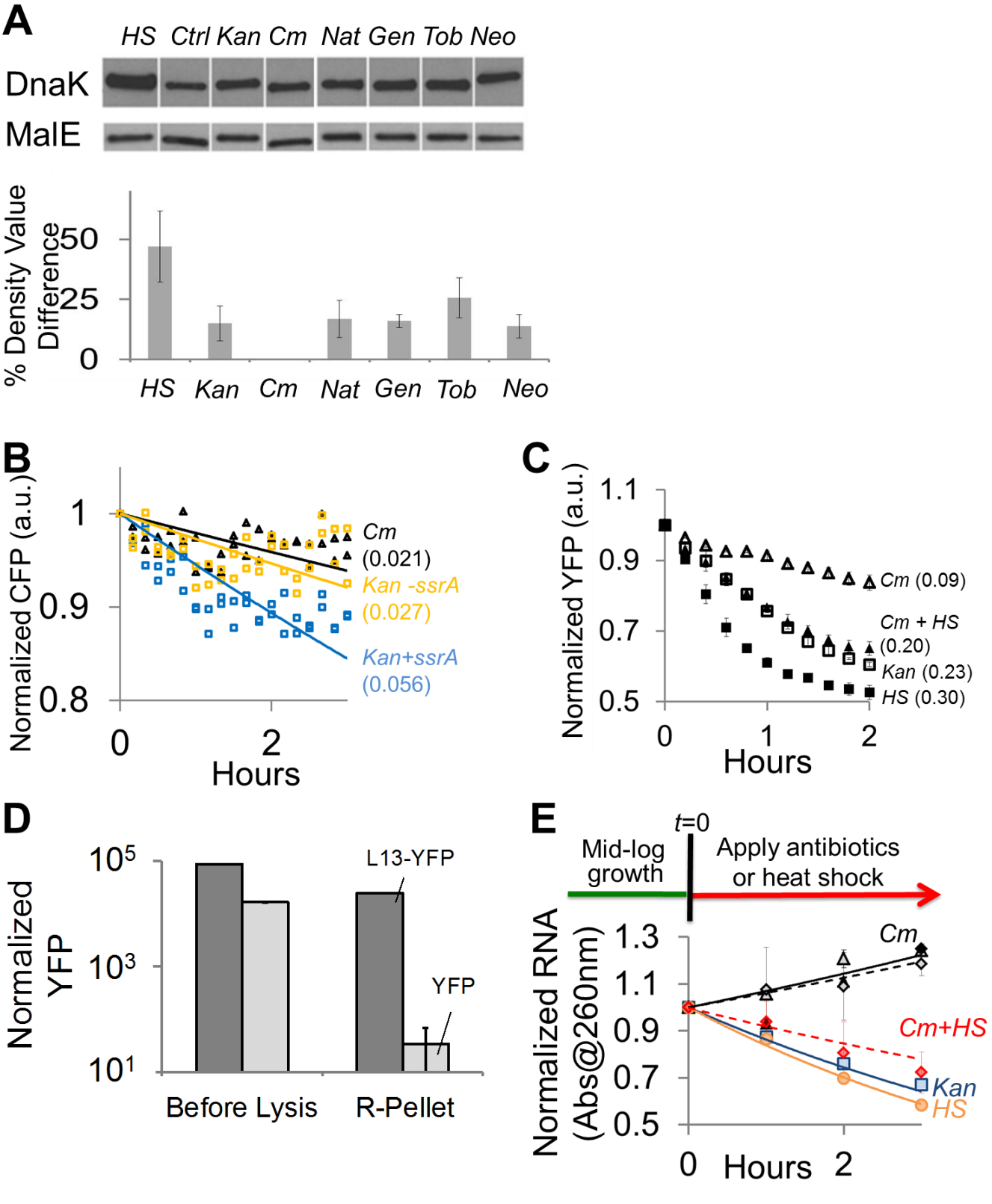
A
HS Ctrl Kan Cm Nat Gen Tob Neo
DnaK
MalE
% Density Value Difference
50
25
0
HS Kan Cm Nat Gen Tob Neo
B
Normalized CFP (a.u.)
1
0.9
0.8
0
2
Hours
Cm (0.021)
Kan -ssrA (0.027)
Kan+ssrA (0.056)
C
Normalized YFP (a.u.)
1.1
0.9
0.7
0.5
0
1
2
Hours
Cm (0.09)
Cm + HS (0.20)
Kan (0.23)
HS (0.30)
D
Normalized YFP
10^5
10^3
10^1
L13-YFP
YFP
Before Lysis
R-Pellet
E
t=0
Mid-log growth
Apply antibiotics or heat shock
Normalized RNA (Abs@260nm)
1.3
1.1
0.9
0.7
0.5
0
Hours
2
Cm
Cm+HS
Kan
HS

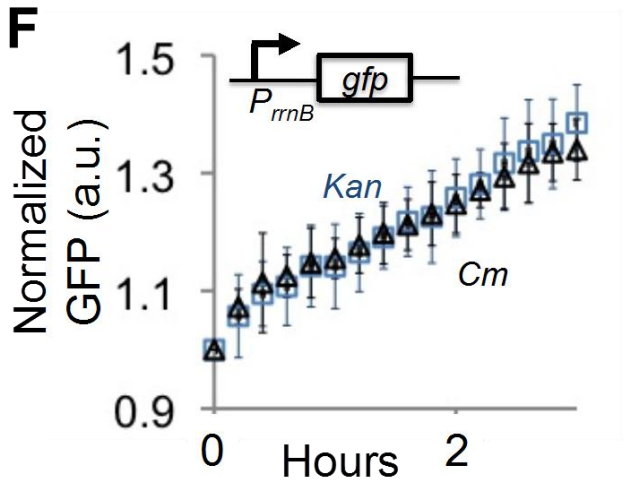
F
Normalized GFP (a.u.)
1.5
1.3
1.1
0.9
0
2
Hours
gfp
P_{rrnB}
Kan
Cm

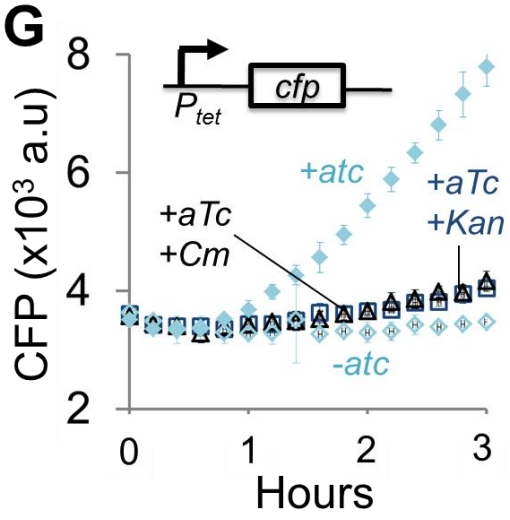
G
CFP (x10³ a.u)
8
6
4
2
0
1
2
3
Hours
cfp
P_{tet}
+atc
+aTc
+Kan
+aTc
+Cm
-atc

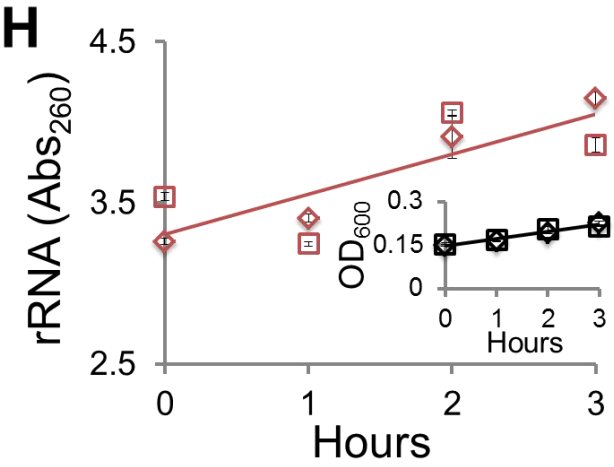
H
rRNA (Abs260)
4.5
3.5
2.5
0
1
2
3
Hours
OD600
0.3
0.15
0
0
1
2
3
Hours

Figure S1: Heat shock response, protein degradation, and RNA degradation in response to antibiotic treatment.

A. Full bacterial extracts from *E. coli* BL21 were subjected to immunoblotting using DnaK antibodies. Treatment with kanamycin (*Kan*), neomycin (*Neo*), nourseothricin (*Nat*), gentamicin (*Gen*), tobramycin (*Tob*) or heat shock (*HS*) resulted in higher levels of DnaK protein when compared to treatment with chloramphenicol (*Cm*) or an untreated culture (*Ctrl*). Protein loading was determined using MalE. The percent difference in density value relative to the *Cm* sample is shown beneath the immunoblot. Each error bar represents standard error of the mean (SEM) calculated using four replicates. A one-way ANOVA analysis suggests that the density values are significantly different between the samples (p-value=0.0178). A paired t-test suggests that the density values are significantly different between all antibiotics with *Cm* (p-value<0.06). See Supplemental Methods for more information.

B. Kanamycin (blue line, 10μg/ml) caused faster degradation of CFP fused with the SsrA-tag than that by chloramphenicol (black lines, 2μg/ml). Kanamycin (yellow line, 10μg/mL) resulted in a similar degradation rate compared to chloramphenicol (CFP contained SsrA-tag) treated cells when CFP lacked an SsrA-tag. Each CFP intensity was normalized by its initial value and the corresponding OD_{600}. Each bracket shows the exponential decay rate ($hour^{-1}$). CFP profiles are significantly different between "*Kan +ssrA*" and chloramphenicol (p-value=0.01), but similar between chloramphenicol and *Kan –ssrA* (p-value=0.7). See Supplemental Methods for more information.

C. Kanamycin (open squares, 10μg/mL) caused faster degradation of ribosomal protein L13 fused to YFP (L13-YFP) than did chloramphenicol (open triangles, 2μg/mL). In addition,

treatment with either heat shock alone (42^{o}C, filled squares) or chloramphenicol (1μg/mL) coupled with heat shock (HS) at 42^{o}C (filled triangles) resulted in faster degradation. Each YFP intensity normalized by OD_{600} is shown relative to its initial value. Each bracket shows the exponential decay rate (hour^{-1}). Data points are representative of the average of three technical replicates in three separate experiments. L13-YPF profiles are significantly between kanamycin and chloramphenicol (p-value=0.0029), chloramphenicol + heat shock and chlorampehnicol (p-value=0.0029), and heat shock and chloramphenicol (p-value=0.0027). See Supplemental Methods for more information.

D. The fusion protein, L13-YFP, is strongly associated with the ribosome. We induced expression of either L13-YFP (dark gray) or a YFP (light gray) only construct in *E. coli* strain BL21pro.The amount of YFP signal from both cell strains prior to lysis was comparable (indicated by 'Before lysis" heading). However, after ribosomes were pelleted by ultracentrifugation, there was a ~500 fold higher amount of normalized YFP signal in the ribosomal pellet isolated from the L13-YFP expressing strain than the YFP expressing control strain (R-pellet heading). 'Before lysis' YFP signal is normalized by Abs600 while the 'R-pellet' YFP value is normalized by Abs260 (rRNA concentration). Values plotted are the average of two experiments. Y-axis is plotted in log scale. See Supplemental Methods for more information.

E. Treatment with kanamycin or heat shock caused faster rRNA degradation than treatment with chloramphenciol. BL21 cultures were treated (t = 0) with kanamycin (100μg/mL, blue line), chloramphenicol (10μg/mL, black line), chloramphenicol (0.7μg/mL, black dotted line), heat shock (at 42^{o}C, orange line), or both chloramphenicol (0.7μg/mL) and heat shock (red dotted line). Each data point is representative of the average of two RNA extractions in a single

experiment (technical replicates) and is plotted relative to the initial value. Results are consistent in two separate experiments. rRNA profiles are significantly different between kanamycin and chloramphenicol, and heat shock and chloramphenicol (p-value<0.05). See Supplemental Methods for more information.

F. The difference in rRNA levels between treatment with kanamycin and chloramphenicol is unlikely due to differences in ribosomal promoter (*rrnB*) activity. To assess ribosomal RNA promoter activity, we used a plasmid that contained the *rrnB* promoter driving the expression of GFP. Treatment with kanamycin (100μg/mL blue line) or chloramphenicol (10μg/mL black line) resulted in identical levels of GFP expression, (normalized by OD_{600}) indicating similar promoter activity under these two conditions. Each data point is representative of three technical replicates of two different clones in two experiments.

G. The *rrnB* promoter analysis described in (F) is not confounded by potential differences in translational inhibition. To assess translational inhibition, we challenged cells with antibiotics that contained a plasmid where the pTet promoter (induced with atc) drove expression of CFP. Treatment with kanamycin (100μg/mL blue line) or chloramphenicol (10μg/mL black line) resulted in identical levels of translational inhibition as determine by identical levels of CFP. As expected, addition of atc to uninhibited cells (no antibiotics, filled light blue diamonds) induced CFP expression. We did not detect CFP expression from cells that were not treated with atc (open light blue diamonds).

H. Total rRNA increases in a growing *E. coli* BL21 culture. We used Abs_{260} to measure total rRNA. Each data point is the average of two RNA extractions in a single experiment (2 technical replicates per experiment). Inset: OD_{600} measurements show that the culture is growing. See Supplemental Methods for more information.

Figure S2

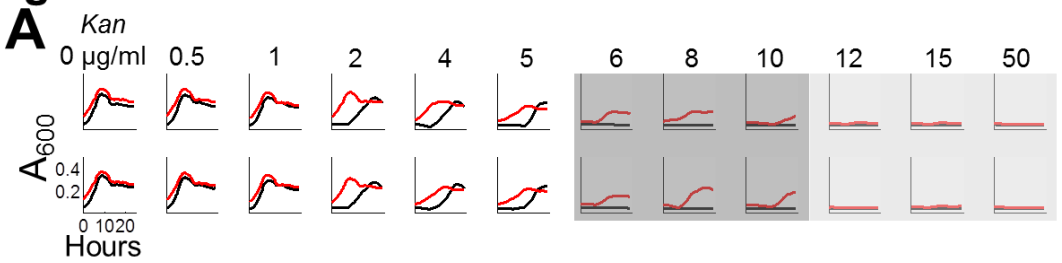
A
Kan
0 μg/ml
0.5
1
2
4
5
6
8
10
12
15
50
A600
0.4
0.2
0 10 20
Hours

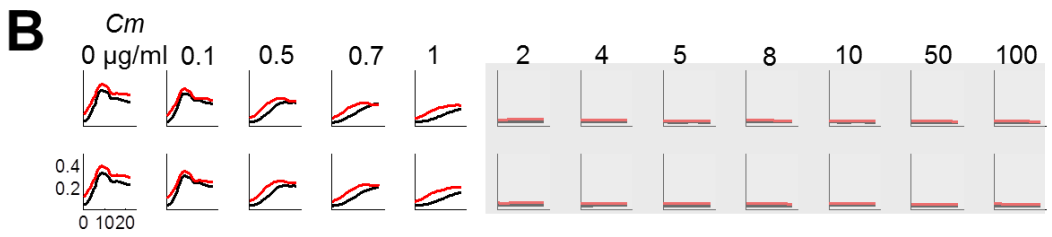
B
Cm
0 μg/ml
0.1
0.5
0.7
1
2
4
5
8
10
50
100
0.4
0.2
0 10 20

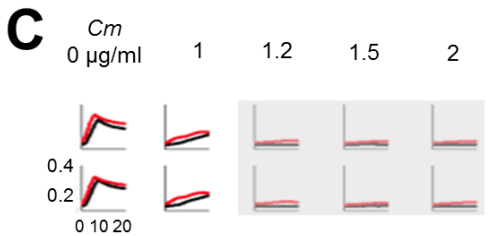
C
Cm
0 μg/ml
1
1.2
1.5
2
0.4
0.2
0 10 20

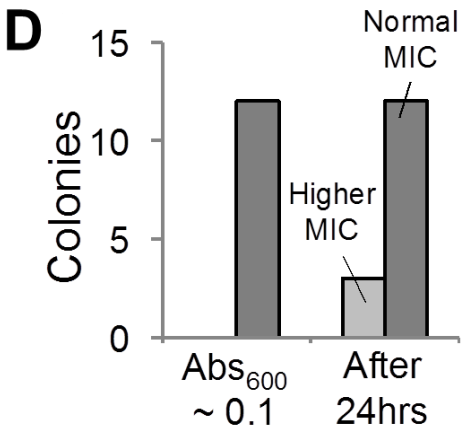
D
Colonies
15
10
5
0
Normal MIC
Higher MIC
Abs600 ~ 0.1
After 24hrs

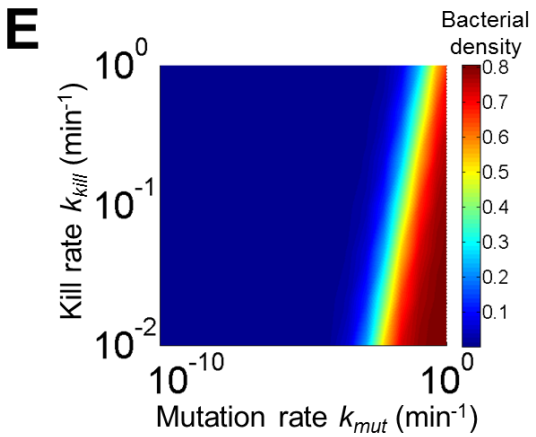
E
Bacterial density
0.8
0.7
0.6
0.5
0.4
0.3
0.2
0.1
Kill rate kkill (min-1)
10^0
10^-1
10^-2
10^-10
10^0
Mutation rate kmut (min-1)

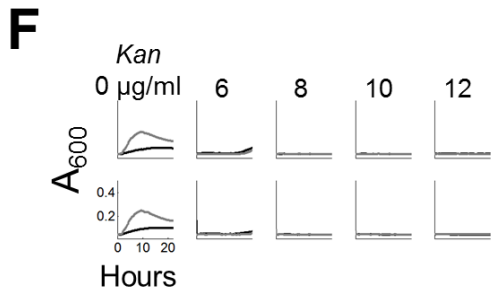
F
Kan
0 μg/ml
6
8
10
12
A600
0.4
0.2
0 10 20
Hours

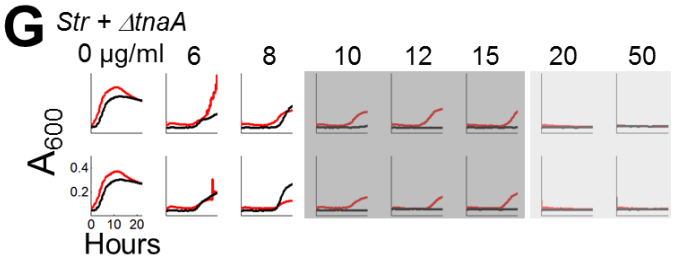
G
Str + ΔtnaA
0 μg/ml
6
8
10
12
15
20
50
A600
0.4
0.2
0 10 20
Hours

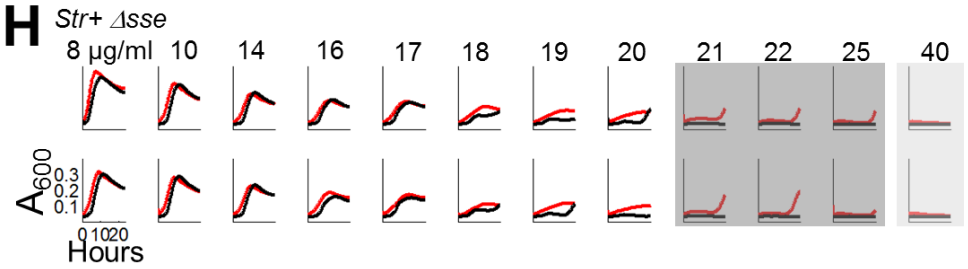
H
Str+ Δsse
8 µg/ml
10
14
16
17
18
19
20
21
22
25
40
A600
0.3
0.2
0.1
0 10 20
Hours

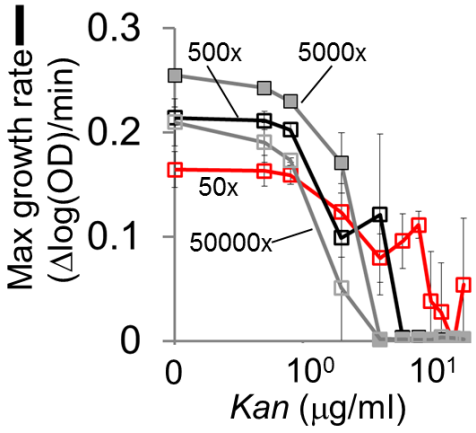
I
Max growth rate
(Δlog(OD)/min)
0.3
0.2
0.1
0
500x
5000x
50x
50000x
0
10^0
10^1
Kan (µg/ml)

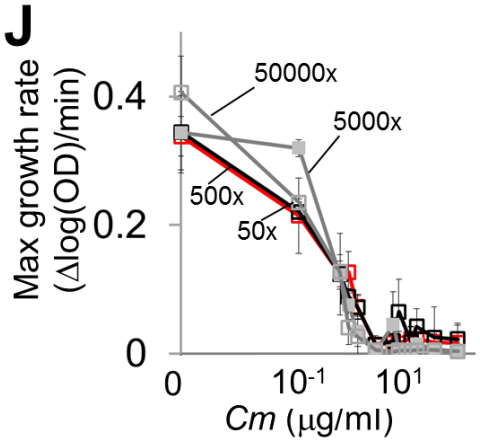
J
Max growth rate
(Δlog(OD)/min)
0.4
0.2
0
50000x
5000x
500x
50x
0
10^-1
10^1
Cm (µg/ml)

Figure S2: IE, which is caused by kanamycin but not chloramphenicol, cannot be accounted for by several alternative resistance mechanisms.

A. Representative growth curves of BL21 challenged with kanamycin. Bacterial populations (*E. coli* strain BL21) exhibited the inoculum effect at 6-10μg/ml kanamycin. We note that CFU measurements are consistent with the OD_{600} measurements. Specifically, at 10μg/ml kanamycin, final CFU of populations with high initial density was ~$5x10^8$ CFU/mL. Whereas final CFU of populations with low initial density was not detected with undiluted cultures (results not shown). Red and black lines represent high and low initial cell densities, respectively. Dark grey regions indicate that populations exhibited IE. Light grey regions indicate that both populations went extinct. In each panel, the upper and lower figures are from two different replicates. CFU was measured following methods described by Kohanski et al., 2007.

B. Representative growth curves of BL21 challenged with chloramphenicol. Bacterial populations (*E. coli* strain BL21) did not exhibit the inoculum effect at all tested concentrations of chloramphenicol

C. Representative growth curves of BL21 challenged with chloramphenicol at concentrations between 1μg/ml and 2μg/ml. Bacterial populations (*E. coli* strain BL21) did not exhibit the inoculum effect at all tested concentrations of chloramphenicol.

D. Spontaneous mutants do not account for growth in IE. We measured the MIC of single colonies grown in kanamycin after reaching Abs600 ~0.1 (10, 8 or 6 μg/ml of kanamycin) or after 24 hours (10μg/ml of kanamycin). In both cases, the majority of single colonies had an MIC that was equal to or lower than BL21 cells that were not previously grown in kanamycin. MICs were assessed using a minimum of two technical replicates.

E. Simulation results of bacterial growth under antibiotic treatment. Biologically feasible mutation rates ($<10^{-8}$resistant cells/cells/min) (Kohanski et al., 2010) could not generate the observed bacterial growth in our experiments.

F. Spent media did not rescue bacteria from kanamycin treatment as populations grown in either spent medium or new medium have the same kanamycin MIC. We removed spent media from cells grown in 0, 6, 8,10 or 12μg/ml kanamycin after six hours. Overnight cultures of BL21 cells were inoculated at 500x into either the spent media or new media. Grey lines represent new media. Black lines represent spent media. Top and bottom panels represent two replicates.

G. *E. coli* BW25113 with *tnaA* knocked out exhibited IE at 10-15μg/ml streptomycin (*Str*). Red and black lines represent high and low initial cell densities, respectively.

H. *E. coli* BW25113 with *sseA* knocked out exhibited IE at 21-25μg/ml streptomycin (*Str*). Red and black lines represent high and low initial cell densities, respectively.

I. Dose response of bacterial growth with increasing concentrations of kanamycin. Red line = 50-fold initial dilution, black line = 500-fold initial dilution, filled grey squares with grey line= 5000-fold initial dilution, and open grey squares with grey line = 50000-fold initial dilution. Each error bar represents one standard deviation of four replicates.

J. Dose response of bacterial growth with increasing concentrations of chloramphenicol.

Figure S3

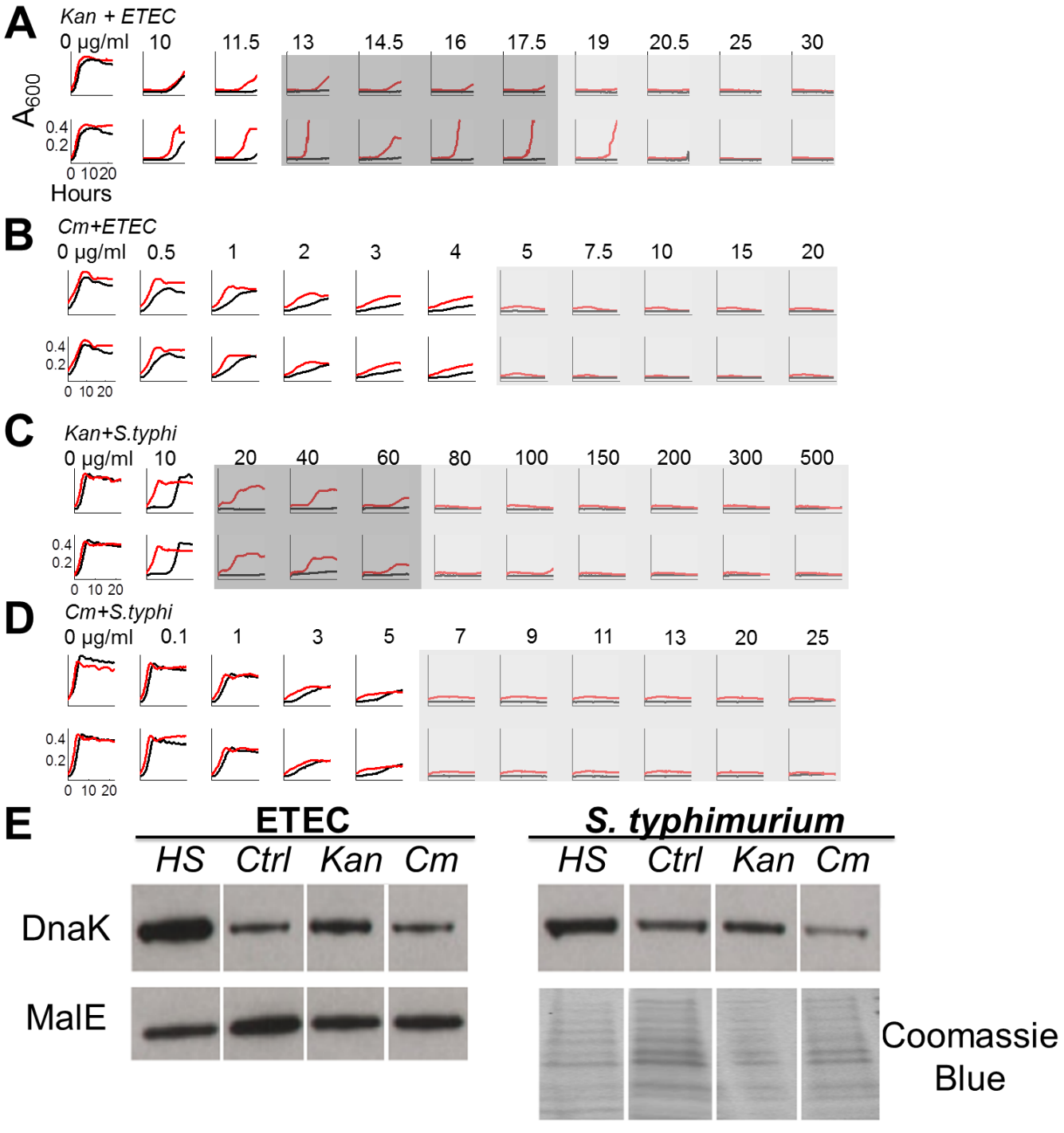
A
Kan + ETEC
0 µg/ml
10
11.5
13
14.5
16
17.5
19
20.5
25
30
A600
0.4
0.2
0 10 20
Hours
B
Cm+ETEC
0 µg/ml
0.5
1
2
3
4
5
7.5
10
15
20
C
Kan+S.typhi
0 µg/ml
10
20
40
60
80
100
150
200
300
500
D
Cm+S.typhi
0 µg/ml
0.1
1
3
5
7
9
11
13
20
25
E
ETEC
S. typhimurium
HS
Ctrl
Kan
Cm
DnaK
MalE
Coomassie Blue

Figure S3: Representative growth curves of ETEC and *S. typhimurium* in varying concentrations of antibiotics.

A. Enterotoxigenic *E. coli* (ETEC) exhibited the inoculum effect at 13-17.5μg/ml kanamycin. Red and black lines represent high and low initial cell densities, respectively. Dark grey regions indicate that populations exhibited IE. Light grey regions indicate that both populations went extinct. In each panel, the upper and lower figures are from two different replicates.

B. Enterotoxigenic *E. coli* (ETEC) did not exhibit inoculum effect at all tested concentrations of chloramphenicol.

C. *S. typhimurium* exhibited the inoculum effect at 20-60μg/ml kanamycin.

D. *S. typhimurium* did not exhibit inoculum effect at all tested concentrations of chloramphenicol.

E. Full bacterial extracts from ETEC and *S. typhimurium* were subjected to immunoblotting using DnaK antibodies. Treatment with kanamycin (*Kan*) or heat shock (*HS*) resulted in higher levels of DnaK protein when compared to treatment with chloramphenicol (*Cm*) or an untreated culture (*Ctrl*). Protein loading was determined using MalE for ETEC and a Coomassie stained duplicate gel for *S. typhimurium*. Similar trends were observed in two independent immunoblots (not shown).

Figure S4

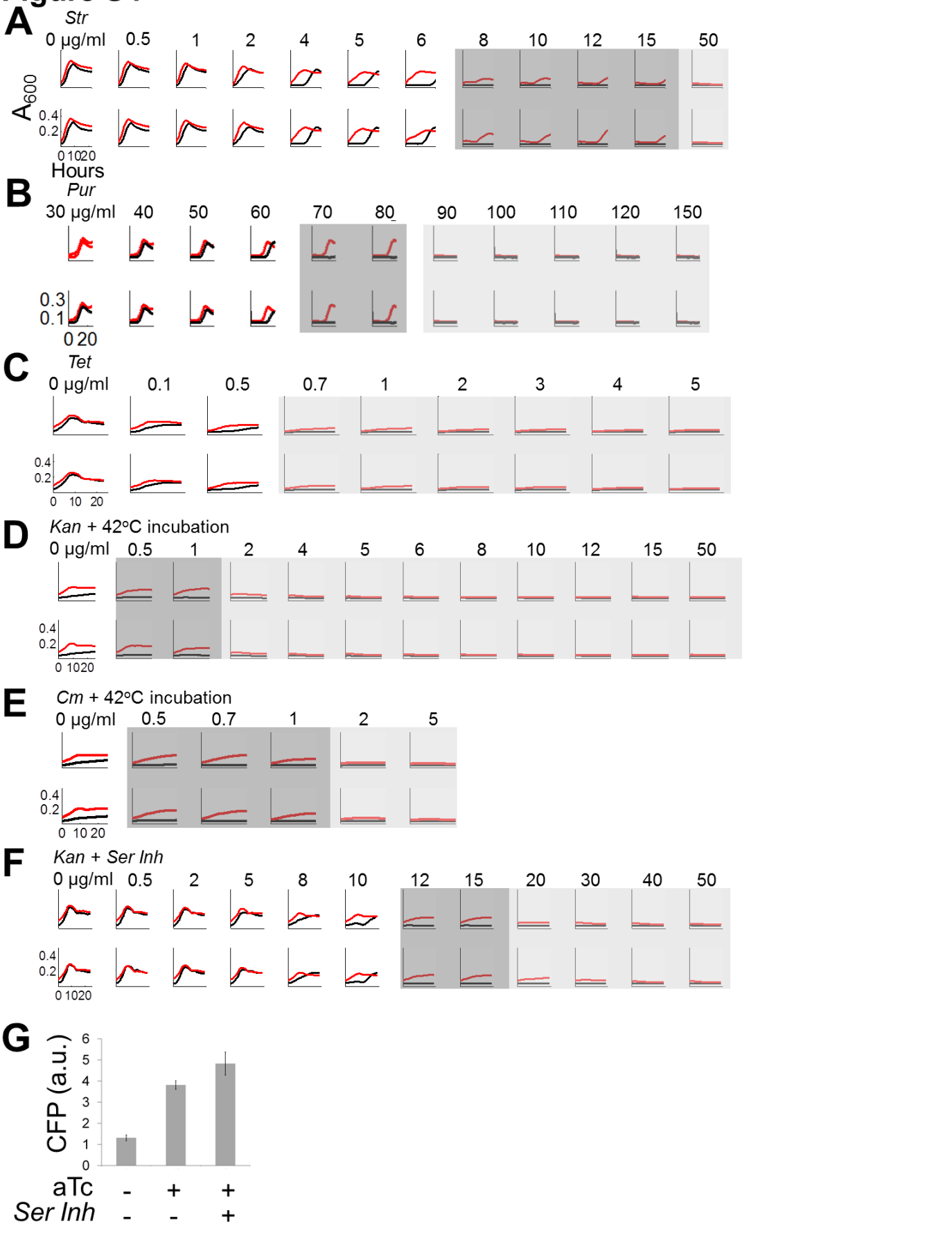
A
Str
0 µg/ml
0.5
1
2
4
5
6
8
10
12
15
50
A600
0.4
0.2
0 10 20
Hours
B
Pur
30 µg/ml
40
50
60
70
80
90
100
110
120
150
0.3
0.1
0 20
C
Tet
0 µg/ml
0.1
0.5
0.7
1
2
3
4
5
0.4
0.2
0 10 20
D
Kan + 42°C incubation
0 µg/ml
0.5
1
2
4
5
6
8
10
12
15
50
0.4
0.2
0 10 20
E
Cm + 42°C incubation
0 µg/ml
0.5
0.7
1
2
5
0.4
0.2
0 10 20
F
Kan + Ser Inh
0 µg/ml
0.5
2
5
8
10
12
15
20
30
40
50
0.4
0.2
0 10 20
G
CFP (a.u.)
0
1
2
3
4
5
6
aTc - + +
Ser Inh - - +

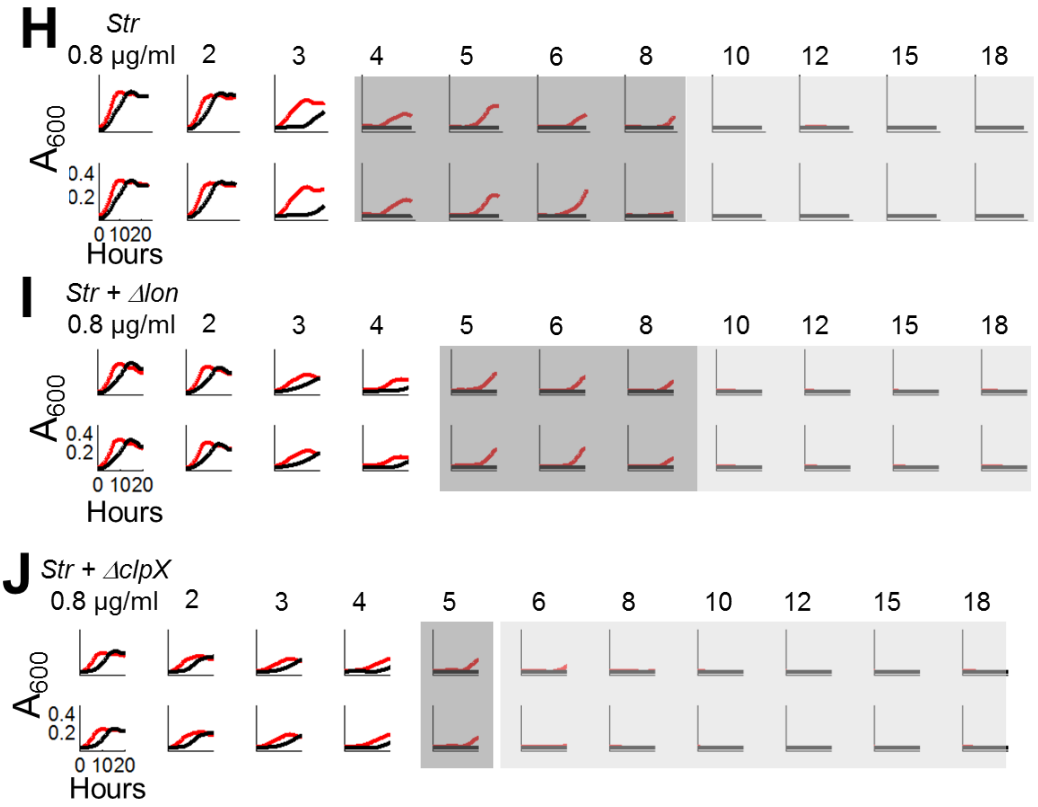
H
Str
0.8 µg/ml
2
3
4
5
6
8
10
12
15
18
A600
0.4
0.2
0 1020
Hours
I
Str + ΔIon
0.8 µg/ml
2
3
4
5
6
8
10
12
15
18
A600
0.4
0.2
0 1020
Hours
J
Str + ΔclpX
0.8 µg/ml
2
3
4
5
6
8
10
12
15
18
A600
0.4
0.2
0 1020
Hours

Figure S4: Representative growth curves of BL21 treated with antibiotics and perturbed with either heat shock or protease inhibitors.

A. Bacterial populations (*E. coli* strain BL21 for all panels) exhibited the inoculum effect at 8-15μg/ml streptomycin. Red and black lines represent high and low initial cell density, respectively. Dark grey regions indicate that populations exhibited IE. Light grey regions indicate that both populations went extinct. In each panel, the upper and lower figures are two different replicates.

B. Bacterial populations exhibited the inoculum effect at 70-80μg/ml puromycin.

C. Bacterial populations did not exhibit the inoculum effect at all tested concentrations of tetracycline. We note that the small increase in OD_{600} was unlikely to be significant because CFU at the 24^{th} hour time point decreased as compared to the initial CFU (results not shown).

D. Bacterial populations exhibited the inoculum effect at 0.5-1μg/ml kanamycin. Microplate cultures were incubated in plate reader at 42^{o}C.

E. Bacterial populations exhibited the inoculum effect at 0.5-1μg/ml chloramphenicol. Microplate cultures were incubated in plate reader at 42^{o}C.

F. Bacterial populations exhibited the inoculum effect at 12-15μg/ml kanamycin when challenged with a serine inhibitor.

G. We demonstrated that the addition of the protease inhibitor increased the concentration of CFP, likely by decreasing overall protein degradation rates. We diluted overnight cultures of BL21Pro/pTetCFP 100-fold into fresh medium supplemented with 100ng/ml anhydro-tetracycline (aTc) and serine protease inhibitor (*Ser Inh*). Specifically, aTc induces CFP

expression from a P_{Tet} promoter and *Ser Inh* inhibits serine proteases. CFP levels were recorded at mid-log phase (OD_{600}~0.1).

H. Bacterial strain BW25113 exhibited the inoculum effect at 4-8μg/ml streptomycin.

I. BW25113 cells with a *lon* knockout exhibited the inoculum effect at 5-8μg/ml streptomycin.

J. BW25113 cells with a *clpX* knockout exhibited the inoculum effect at 5μg/ml streptomycin.

Figure S5

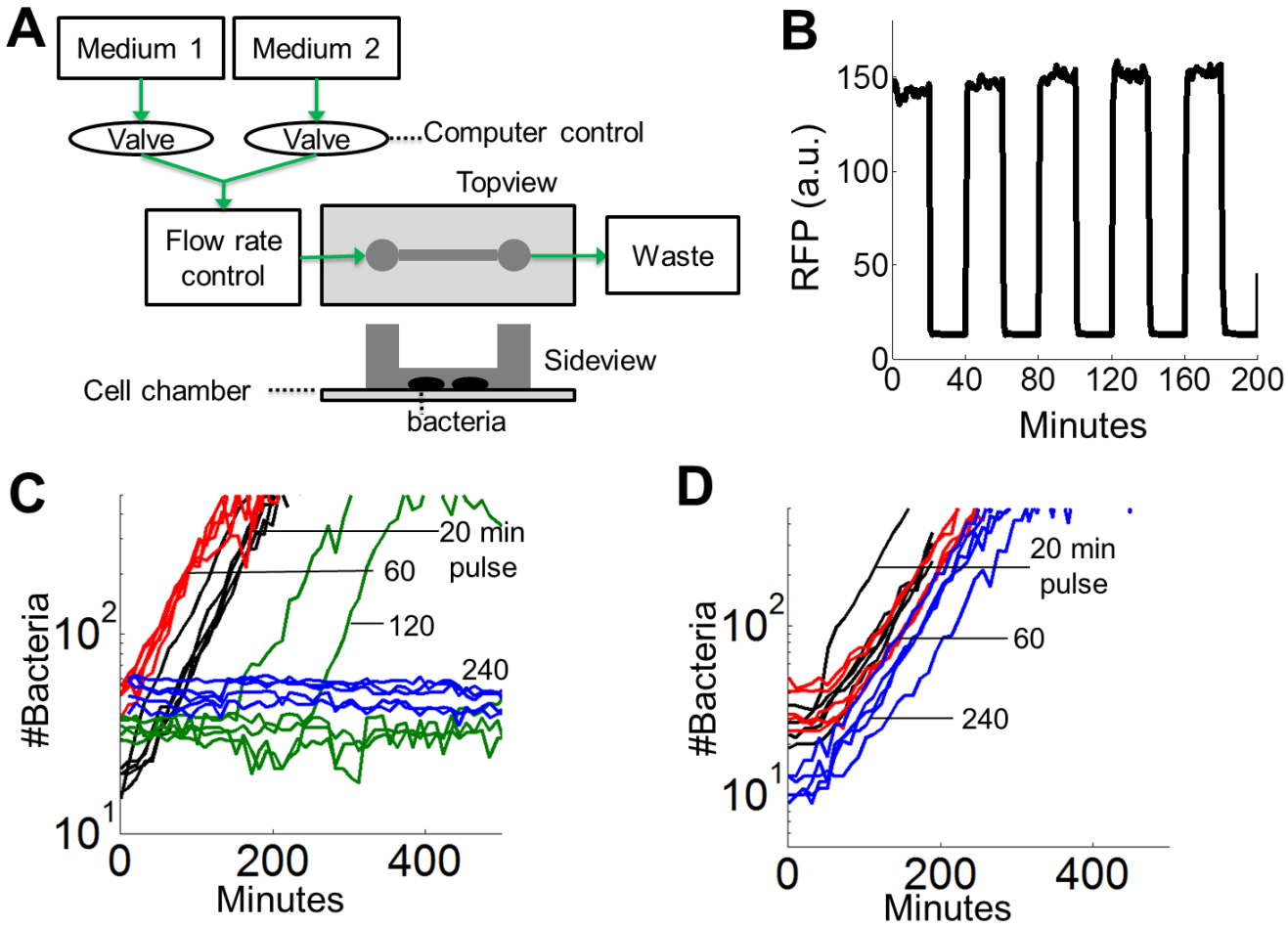
A
Medium 1
Medium 2
Valve
Valve
Computer control
Topview
Flow rate control
Waste
Sideview
Cell chamber
bacteria
B
RFP (a.u.)
150
100
50
0
0
40
80
120
160
200
Minutes
C
#Bacteria
10^2
10^1
0
200
400
Minutes
20 min pulse
60
120
240
D
#Bacteria
10^2
10^1
0
200
400
Minutes
20 min pulse
60
240

Figure S5: Calibration of the flow system and recovery of bacterial populations from transient antibiotic treatment.

A. A flow system for analyzing bacterial growth in oscillating environments.

B. Medium with and without sulforhodamine was alternated at a pulse period of 40 minutes. Red fluorescence dynamics followed the pulse period closely.

C. Bacterial recovery from treatment with 10μg/ml kanamycin. Bacterial recovery was heterogeneous with the treatment duration of 120min, likely because it was near to a critical duration when populations could not recover. Such heterogeneity, however, would not affect the band-pass response to periodic treatment (Figure 7C). Each time series represents population growth in one microscope field.

D. Bacterial recovery from treatment with 10μg/ml chloramphenicol.

Figure S6

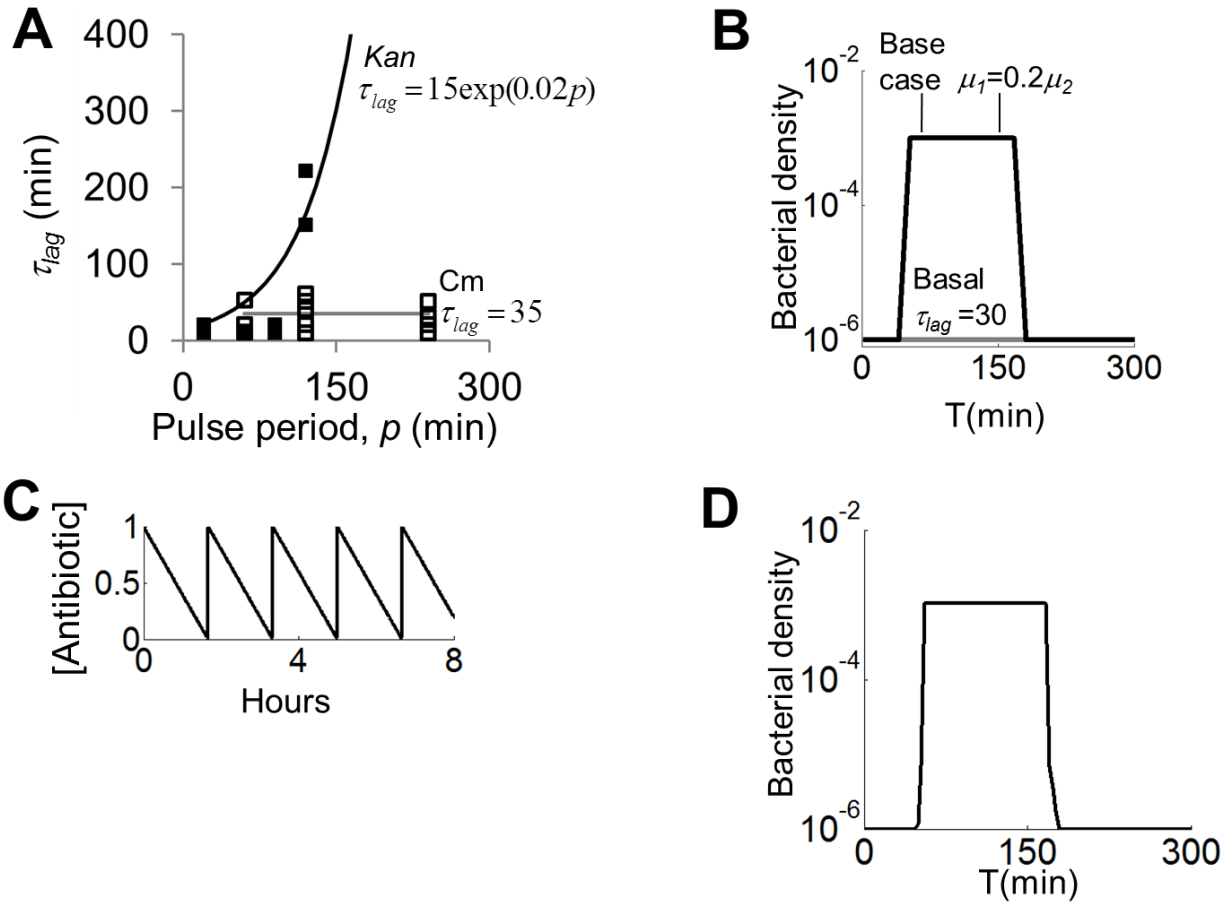
A
400
300
200
100
0
τ_{lag} (min)
Kan
$\tau_{lag} = 15\exp(0.02p)$
Cm
$\tau_{lag} = 35$
0
150
300
Pulse period, p (min)
B
Base case μ_1=0.2μ_2
10^{-2}
10^{-4}
10^{-6}
Bacterial density
Basal
τ_{lag} =30
0
150
300
T(min)
C
[Antibiotic]
1
0.5
0
0
4
8
Hours
D
10^{-2}
10^{-4}
10^{-6}
Bacterial density
0
150
300
T(min)

Figure S6: Perturbation of the simplified model

A. Based on our experimental results, we assumed that recovery time increases exponentially with kanamycin (black line) and stays constant with chloramphenicol (grey line). Even though we could not fit the recovery time perfectly with an exponential function, the function gave rise to the band-pass response (Figure 6B) that was consistent with experimental results (Figure 7). Data points (both open and filled squares) are the same as presented in Figure 5C.

B. For the base case, $\mu_1 = \mu_2$ and basal τ_{lag} is 15min. The region of band-pass response stayed constant with a smaller μ_1 ($=0.2\mu_2$). The region of band-pass response diminished with an increased basal τ_{lag} (=30min). Total simulation time was 24 hours.

C. An antibiotic decay profile was simulated by using a sawtooth function in Matlab.

D. The inclusion of the antibiotic decay function does not change the qualitative nature of our modeling predictions. Specifically, with IE, bacterial growth is maximized at intermediate pulse periods.

Figure S7

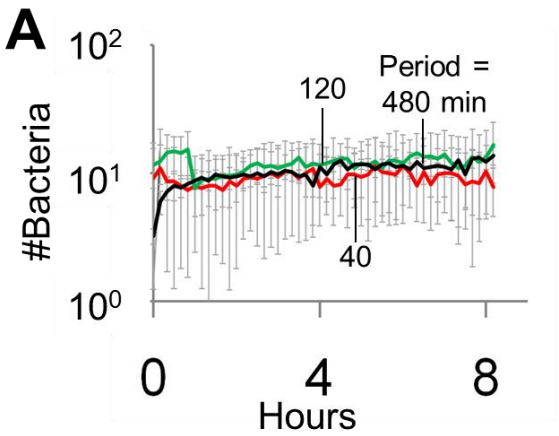
A
10^2
10^1
10^0
#Bacteria
120
Period =
480 min
40
0
4
8
Hours

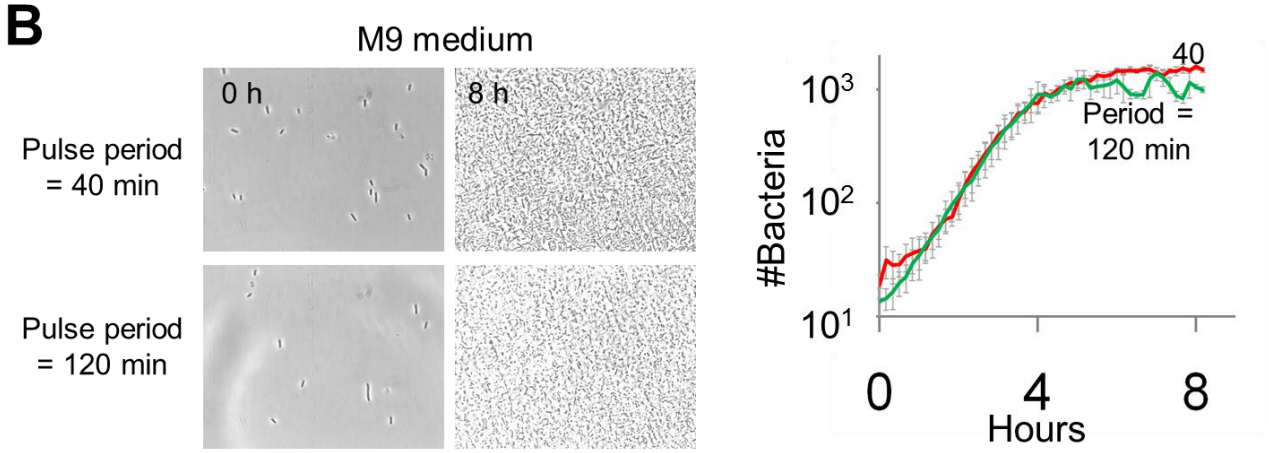
B
M9 medium
Pulse period
= 40 min
Pulse period
= 120 min
0 h
8 h
10^3
10^2
10^1
#Bacteria
40
Period =
120 min
0
4
8
Hours

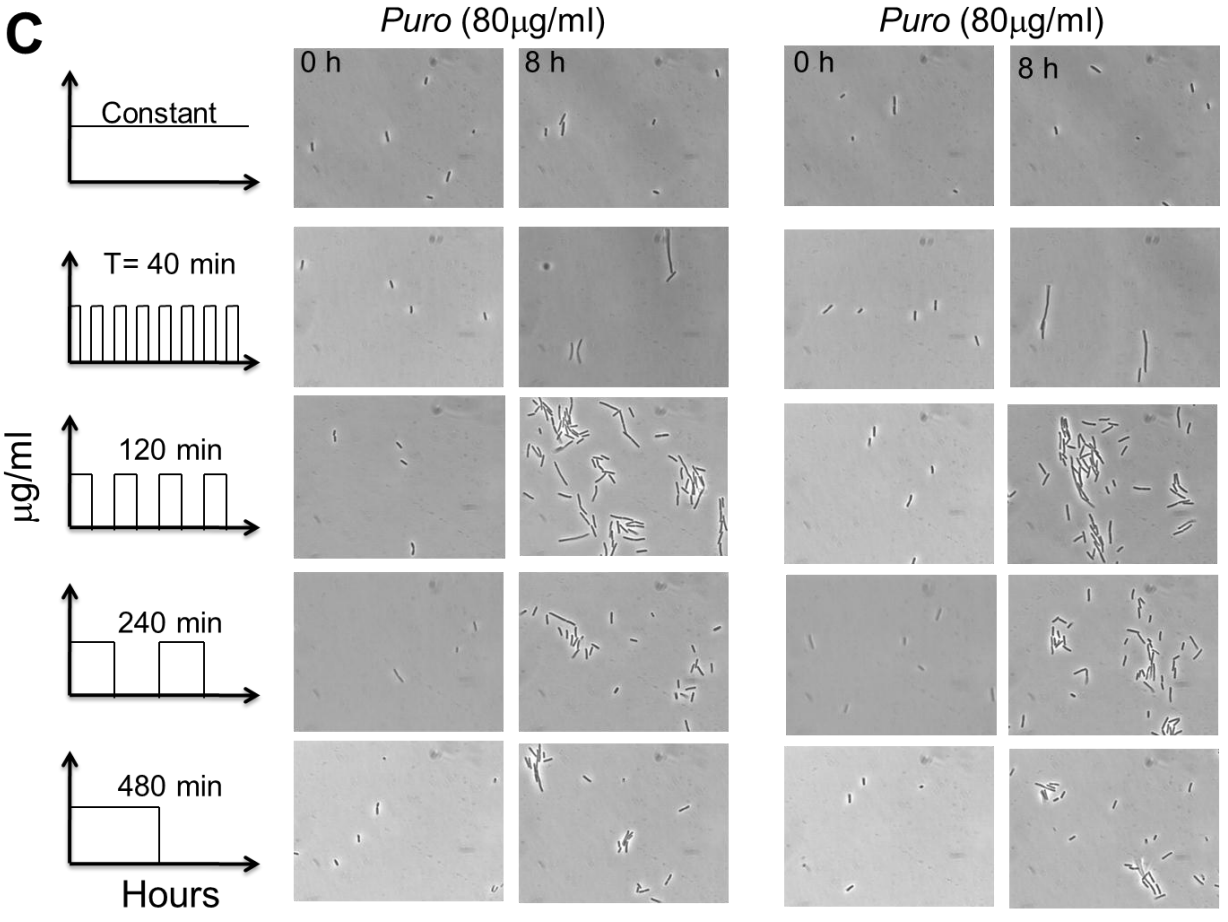
C
Puro (80μg/ml)
Puro (80μg/ml)
0 h
8 h
0 h
8 h
Constant
T= 40 min
120 min
240 min
480 min
μg/ml
Hours

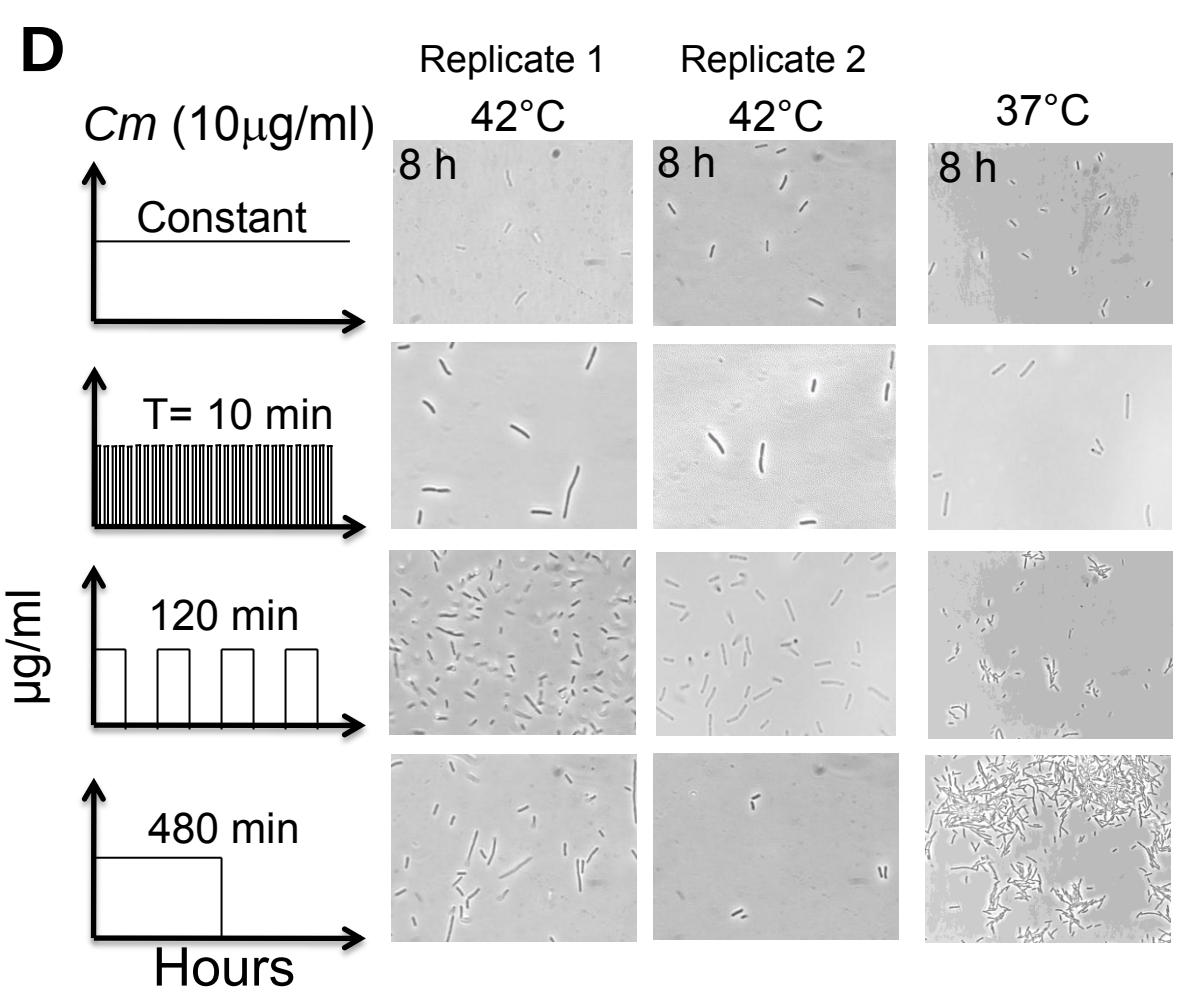
D
Replicate 1
Replicate 2
42°C
42°C
37°C
Cm (10μg/ml)
Constant
T= 10 min
120 min
480 min
μg/ml
Hours
8 h
8 h
8 h

Figure S7: Bacterial growth during pulsatile antibiotic treatment.

A. Bacterial growth in three pulse periods of M9 medium supplemented with 20μg/ml kanamycin.

B. Representative bacterial growth in two pulse periods of blank M9 medium. Bacterial densities were not affected by the pulse period of 40 minutes, which was the fastest pulse period applied in our experiments (Figure 7). Each error bar indicates one standard deviation of five images. Representative time series were obtained from two independent experiments.

C. Representative bacterial growth with periodic puromycin (80μg/ml) treatment. At the 8^{th} hour, bacterial densities peaked at an intermediate pulse period (120 minutes).

D. Representative bacterial growth with periodic chloramphenicol (10μg/ml)) treatment at 42^{o}C (heat shock) and 37^{o}C. In the presence of heat shock, the bacterial density peaked at an intermediate pulse period of 120 minutes, at 8^{th} hour after inoculation. In the absence of heat shock, bacterial density increased with longer pulse period. Two replicates of chloramphenicol and heat shock treatment are shown.